

**NEW GENERATION MODELING AND DECISION SUPPORT TOOLS
FOR STUDYING IMPACTS OF DAM FAILURES**

Mustafa S. Altinakar, PhD ¹

Enrique E. Matheu, PhD ²

Marcus Z. McGrath ³

ABSTRACT

Dams and levees are one of the eighteen Critical Infrastructure and Key Resource sectors identified by the National Infrastructure Protection Plan. Failure of dams could lead to highly dynamic, catastrophic floods that could potentially cause loss of life, urban and agricultural property damage, environmental degradation, and cascading failures in other critical sectors. Predicting and assessing these potential impacts are therefore important, and there is a clear need for cost-effective methods, tools and technologies for studying the impacts of dam failures based on new technologies.

Recent developments in conservative, shock capturing finite volume methods to solve shallow water equations in case of mixed-regime flows over complex topographies opened up new

¹ Associate Director and Research Professor, National Center for Computational Hydroscience and Engineering, The University of Mississippi; altinakar@ncche.olemiss.edu

² Chief, Dams Sector Branch, SSA Executive Management Office, Office of Infrastructure Protection, U.S. Department of Homeland Security; enrique.matheu@dhs.gov

³ Graduate Student, National Center for Computational Hydroscience and Engineering, The University of Mississippi; mzmcgrat@ncche.olemiss.edu

avenues for robust and realistic two-dimensional (2D) simulation of dam/levee break breaching floods. In current practice, these simulations are often carried out using one-dimensional (1D) models, which cannot capture the dynamics of highly dynamic floods resulting from the failure of dams, especially when the terrain is flat and the flow is not channelized.

Considerable advances in geographic information systems (GIS) and remote sensing technologies have facilitated the data preparation for 2D models. Digital elevation maps and remote sensing images can be used efficiently to set up 2D simulations of failure scenarios. The results obtained from 2D models can be directly imported into a GIS platform and be effectively interfaced with various geospatial socio-economic data layers to study flood impacts, such as loss of life, downstream property damage, etc.

This paper describes an integrated environment to study the impacts of dam failures by combining a state-of-the-art 2D simulation model with a GIS-based decision support system to support comprehensive risk assessments. Examples of application of this integrated environment to some practical problems are also presented.

INTRODUCTION

The National Inventory of Dams currently maintains records for 82,642 dams, of which 73,898 are earth embankments. Roughly 11,881 dams are high-hazard, and 13,549 are significant hazard dams. Close to half of the high-hazard and significant hazard dams do not yet have an Emergency Action Plan. Therefore, it is of great importance to develop robust and accurate numerical models coupled with decision support systems that utilize recent developments in numerical modeling, computer hardware, and geographic information systems (GIS) and remote sensing technologies to provide the engineers with cost- and time-effective tools to perform risk and vulnerability studies by carrying out realistic dam-break simulations for various failure scenarios and assessing consequences.

A large number of numerical models are available for computation of dam break flows.

Generally, the existing models can be categorized into one of the following categories:

1. Simplified numerical models aimed at determining the envelope maximum water depths based on some hydrologic modeling and/or by filling a digital map with a volume equal to a portion or total of the water stored in the reservoir.
2. One-dimensional (1D) models that solve either full dynamic or simplified forms of conservative or non-conservative 1D, cross-section averaged, shallow water equations (i.e., Saint-Venant equations).
3. Two-dimensional (2D) models that solve either full dynamic or simplified forms of conservative or non-conservative 2D shallow water equations.

4. Coupled (or integrated) 1D-2D models that solve both one-dimensional channel flow and two-dimensional overland flow together using full dynamic or simplified forms of conservative or non-conservative one- and two-dimensional shallow water equations. A coupled model may take into account either the mass exchange only or both mass and momentum exchanges between 1D and 2D models.

In current engineering practice, mostly 1D models are used for dam break studies, even in situations where the underlying assumptions of 1D modeling are clearly violated and the use of a 2D model is warranted. The most common objections against the use of 2D models are: 1) long computational times; 2) the necessity to generate topographic mesh, which can consume considerable time and effort; and 3) tedious and lengthy input data preparation.

It can be confidently argued that the above objections to the use of 2D models for flood studies are no longer valid. Recent scientific and technological developments have completely changed that outlook. First, recent advances in conservative numerical solutions of hyperbolic equations with shock capturing capability have permitted the development of robust numerical codes to solve shallow water equations for mixed regimes over a realistic topography. Second, the improvements in computer hardware (processor speed, storage capabilities, parallel and/or cluster computing, networking, etc.) make it possible to simulate even relatively large areas – for example, 75km by 75km, at a resolution of 50m s on a personal computer in a matter of several hours. Finally, recent developments in remote sensing and measuring methods and GIS technologies have facilitated the collection, treatment, storage, and retrieval of enormous amounts of geospatial data (topography, land cover, roughness, etc.) needed for realistic simulations when using 2D models. Technology has reached a level that allows the engineer to

choose the right type of model for the problem at hand and the amount of data available, rather than to reformulate the problem so that it can be solved with the available modeling capabilities.

Undoubtedly, 1D unsteady flow models have several attractive features. Experience has shown that, when appropriately used, 1D models can provide reliable results even in relatively complex problems. Simulations generally run faster; however, preparation of the cross-section data may take considerable time and, in some cases, engineering judgment may be required to select the location of cross-sections and their width. Considerable level of expertise accumulated in the engineering community regarding the use of 1D models is also an important factor.

However, in practice, one encounters many situations where 1D models are not appropriate. Errors may arise when the dam is very high and the initial water difference between upstream and downstream is large. Many 1D unsteady flow models used in engineering practice cannot handle mixed flow regimes that can be present in highly dynamic dam-break floods. Sudden changes in cross-section (contractions or expansions) may constitute a serious challenge for many existing 1D models (problems of instability). The 1D model, which assumes that the flow reaching a cross-section takes up as much width as it can, cannot provide sufficiently accurate results when the flow is not channelized or the dam-break flood propagates on a flat terrain.

One of the critical shortcomings of 1D models is that they only provide a water surface elevation (depth) and a discharge at the computational cross-sections along the river. In order to obtain a 2D map of the inundated area, 1D model results must be converted into 2D maps by interpolating between 1D model cross-sections based on digital elevation maps. Determination of flood levels in the tributaries requires additional computations and further interpolations.

Although this standard procedure may give sufficiently good results for slowly rising and falling fluvial floods, it may lead to serious errors in cases involving highly unsteady dam-break floods, especially over relatively flat terrain, and thus violate the conservation of mass.

BRIEF REVIEW OF SOME EXISTING MODELS

Simplified Models

An example of the simplified numerical model is the “Simplified Dam-Break” (SMPDBK) model developed by the National Weather Service (NWS) for predicting downstream flooding produced by a dam failure. The SMPDBK model does not provide time-varying results for a dam break simulation, nor does it account for backwater effects created by channel constrictions, downstream dams or bridge embankments. The model is useful for situations where a rapid estimation of areas to be flooded by a dam break is necessary and only limited data is available. The input required for a SMPDBK model is a stream centerline, cross-sections, and information regarding the storage and failure of the dam being modeled. WMS (The Watershed Modeling System) software can be used to prepare the input file for SMPDBK and to launch the computation. After completion, WMS automatically reads the results and creates a water surface elevation data set for automated floodplain delineation.

1D Models

The Full Equations (FEQ) computer program (Franz and Melching, 1997) simulates flow in a stream system by solving the full equations of motion for 1D, subcritical unsteady flow. The

effect and/or operation of structures including bridges, culverts, dams, spillways, weirs, and pumps may be simulated with the program. A companion program (FEQUTL) operates as a pre-processor to convert cross-section data into hydraulic tables for use during unsteady computations. The FEQ program uses continuity and momentum equations to determine the flow and depth throughout the stream system following the specification of initial flow and boundary conditions. FEQ was initially developed for simulation of flow through the Sanitary and Ship Canal in Chicago, Illinois. It is not particularly adapted for dam break simulations.

Developed in the late 1980s by NWS, FLDWAV is a combination of two popular NWS programs: the Dynamic Wave Operation Network Model, developed by Fread (1982), and the Dam-Break Forecasting Model, developed by Fread (1984). The FLDWAV solves full dynamic Saint-Venant equations for real-time forecasting of natural floods or dam-break events in dendritic channel networks. The flow can be subcritical or supercritical. Mixed flows are handled by automatically dividing the simulated channel into sub-reaches of unique flow regime. The FLDWAV handles levee overtopping and breaching, split flow (island) situations, bridges, and the modeling of mud-debris flow. The FLDWAV model has been used in numerous dam-break simulations to estimate the maximum crest height and warning time available for downstream inhabitants. Planned future improvements include the addition of culvert modeling, movable gate operations, sediment transport, new routing methods, and modeling of landslide-generated waves in reservoirs.

The most popular and widely used model for steady backwater computations is the HEC-RAS model. Among other capabilities, it now also provides the unsteady flow capability using the same set of geometry data. Unsteady flow computations use the full equations of motion (St.

Venant equations) when the flow is either subcritical or supercritical over the entire length.

Mixed flows are handled by reverting gradually to diffusive wave equation as the Froude number approaches a user defined critical value. Although the unsteady flow equation solver is taken directly from the HEC-UNET, other unsteady flow procedures in HEC-RAS are different from those in HEC-UNET. A post-processor facilitates the output review and provides all the tables and plots for unsteady flow that are available for steady flow computations. Without the post-processor, only graphical output consisting of stage and/or discharge hydrographs at all cross-sections is available. Unsteady HEC-RAS includes dam breaching, levee break algorithms, and modeling of pumping stations. As is the case when modeling steady flow in HEC-RAS, the unsteady analysis is limited to 500 profiles. A maximum of 6,000 cross-sections may be used in the model, with up to 500 elevation-station points for each cross-section. In unsteady flow analysis, a set of curves is developed for defining the headwater-tailwater discharge relationships through each obstruction, such as bridges and culverts, for a full range of flow.

Developed by Wallingford Software, ISIS Flow can simulate gradually unsteady flows in channels by solving full dynamic unsteady flow equations using the Preissmann implicit scheme. It can handle complex looped and branched networks. ISIS Flow incorporates both unsteady and steady flow solvers, with options that include simple backwaters, flow routing and full unsteady simulation.

2D Models and Coupled 1D-2D Models

Although a large number of 2D unsteady models are available, only a small number of them can handle mixed flows and wetting and drying. Some of the recently developed models also offer

the capability of coupled 1D-2D simulation, which allows the user to take advantage of both 1D and 2D modeling. A few selected models are briefly mentioned below.

FESWMS is a hydrodynamic modeling code that supports both super and subcritical flow analyses, including area wetting and drying. It has been developed under funding by the U.S. Federal Highways Administration by Froelich (2002). FESWMS is specifically suited for modeling regions involving flow control structures, such as those encountered at the intersection of roadways and waterways. Specifically, the FESWMS model allows the user to include weirs, culverts, drop inlets, and bridge piers into a standard 2D finite element model. SMS provides graphical tools for defining these structures and controlling analysis using the FESWMS model. Both pre- and post-processing capabilities are included in the interface.

Developed by DHI Group in Denmark, MIKE FLOOD is a commercially available integrated tool for floodplain studies. It combines the two numerical hydrodynamic models MIKE 11 (1-D) and MIKE 21 (2-D) with a unified user interface. It can be used for various unsteady flood applications such as fluvial flooding, storm surge, dam break, embankment failure, etc.

BASEMENT is a numerical simulation software developed at the Laboratory of Hydraulics, Hydrology and Glaciology of the Swiss Federal Institute of Technology in Zurich, Switzerland. The purpose of the software, which is publicly available, is to provide a software tool for numerical modeling of environmental flow and natural hazard events.

Especially popular in the United Kingdom and Australia, TUFLOW is a 1D and 2D flood and tidal flow simulation software that solves full dynamic equations of unsteady flow. It also

provides coupled 1D-2D simulations by linking 1D and 2D models. TUFLOW has been merged with XP-SWMM 1D engine by XP-Software and GUI, ISIS 1D engine developed by Halcrow.

Developed by the University of Mississippi's National Center for Computational Hydroscience and Engineering (NCCHE), CCHE2D is an integrated package for 2D simulation and analysis of river flows, non-uniform sediment transport, morphologic processes, coastal processes, pollutant transport and water quality on a quadrilateral mesh. These processes are solved with the depth-integrated Reynolds equations, transport equations, sediment sorting equation, bed load and bed deformation equations. CCHE2D is based on the Efficient Element Method, a collocation approach of the Weighted Residual Method. Internal hydraulic structures, such as dams, gates and weirs, can be formulated and simulated synchronously with the flow. Dry and wet capability enables one to easily simulate flows with complex topography. Three turbulence closure schemes are available. The numerical scheme can handle mixed flows. CCHE2D has also a mesh generator and a complete Graphic User Interface (GUI) for pre- and post-processing.

Also developed by NCCHE, CCHE2D-FLOOD is a 2D numerical model that solves full dynamic unsteady flow equations over a regular Cartesian mesh (such as a DEM) using a shock capturing upwind finite volume scheme. CCHE2D-FLOOD can handle mixed flow regimes and wetting and drying. It also offers coupled 1D-2D modeling using a special version of cut-cell boundary technique. CCHE2D-FLOOD is integrated with GIS-based Decision Support System for Water Infrastructural Security (DSS-WISE), which provides pre-processing for input data preparation and post-processing for consequence analysis and risk and vulnerability studies.

REVIEW OF HYDRODYNAMICS OF DAM BREAK FLOW

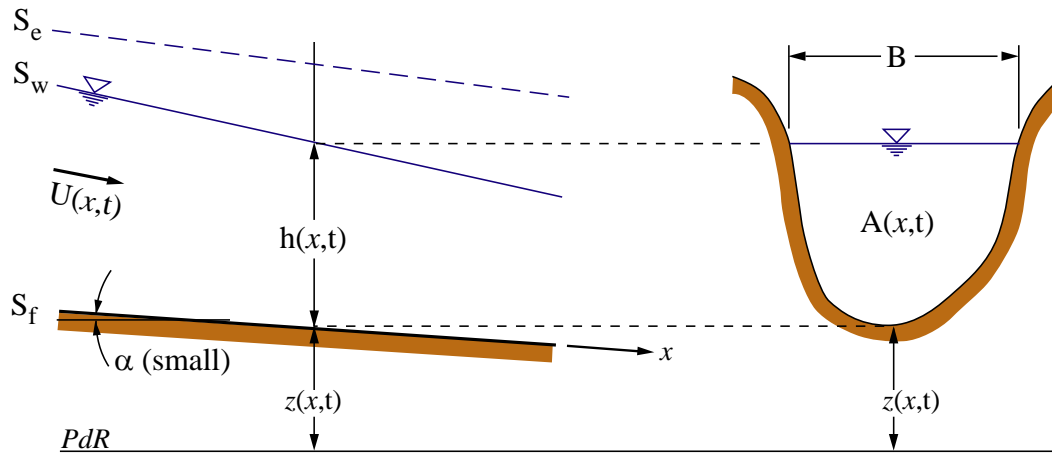


Figure 1. Definition sketch of an unsteady free surface flow in an open channel

Unsteady free-surface flow in an open channel with fixed bed is described by Saint-Venant (or shallow-water) equations (Chanson, 2004), as:

$$\frac{\partial A}{\partial t} + \frac{\partial Q}{\partial x} = q_\ell \quad (1a)$$

$$\frac{\partial Q}{\partial t} + \frac{\partial}{\partial x} \left(\frac{Q^2}{A} \right) + gA \frac{\partial h}{\partial x} = -gA \frac{\partial z_b}{\partial x} - g \frac{Q|Q|}{C^2 R_h A} \quad (1b)$$

where A is the wetted cross section area, h the local flow depth, R_h the hydraulic radius, $Q = VA$ the discharge with V being the average velocity, q_ℓ the lateral discharge (which is a volume source or sink per unit length per unit time), g the gravitational acceleration, z_b the elevation of channel invert, and C represents the Chezy coefficient of roughness. Equations 1a

and 1b represent the conservation of mass and momentum, respectively, and they are valid for unsteady flow in both prismatic and non-prismatic channels. The Saint-Venant (or shallow water) equations on a fixed bed are derived with the assumption that the flow is 1D, the streamline curvature is very small, the pressure is hydrostatic (i.e., vertical accelerations are neglected), and the bed slope is small. Furthermore, it is assumed that the friction loss can be expressed in the same way as in uniform flow, per the Chezy equation.

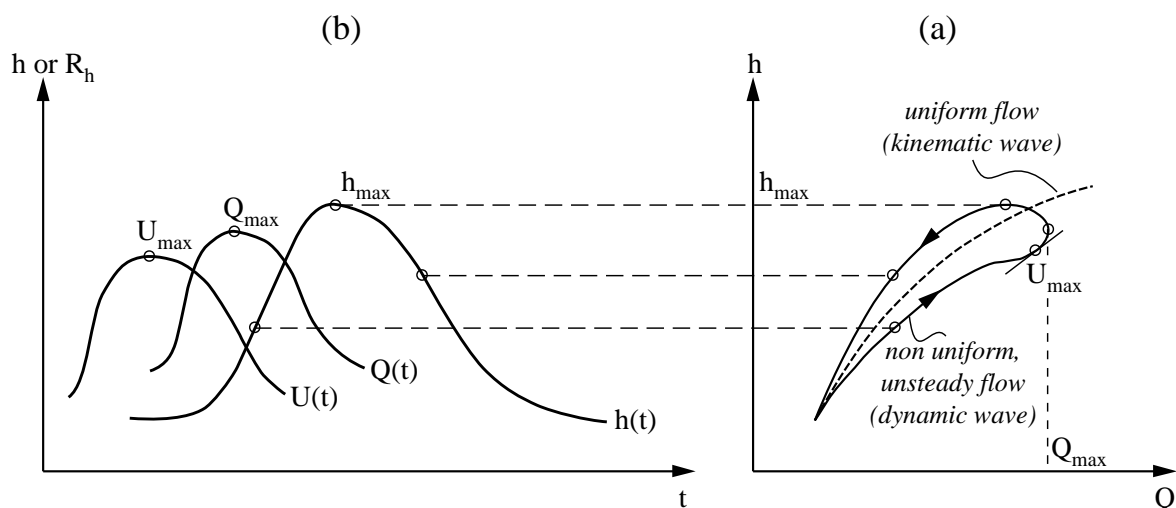


Figure 2. Hysteresis effect in unsteady open channel flow

An important characteristic of unsteady flow is the hysteresis effect shown in Figure 2. At a given station, the maximum values of velocity, discharge and depth does not occur at the same time. The stage discharge curve is not monotonic (or single-valued) as in the case of uniform flow, but displays a hysteresis effect (i.e., the same discharge can occur at different heights depending on rising and falling limbs of the hydrograph). It is important to note that in the case of real rivers, changes in cross-section and other effects may lead to a hysteresis curve more complex than the theoretical shape shown in Figure 2.

The form of the momentum equation given in Equation 1b corresponds to full dynamic unsteady flow. Simpler forms of this equation can be obtained by neglecting different combination of terms. Table 1 shows all possible combinations used in practice and briefly comments on their use and limitation (Graf and Altinakar, 2002).

$\frac{\partial Q}{\partial t} + \frac{\partial}{\partial x} \left(\frac{Q^2}{A} \right) + gA \frac{\partial h}{\partial x} = 0$	Simple wave: Represents the special case of unsteady flow of an ideal (inviscid) fluid over a horizontal bed.
$0 = -gA \frac{\partial z_b}{\partial x} - g \frac{Q Q }{C^2 R_h A}$	Kinematic wave: Acceleration and inertial terms are neglected and free surface is taken as parallel to the bottom. It can be considered as a succession of uniform flows with different discharges. The kinematic wave does not attenuate and there is no hysteresis. It cannot take into account backwater effects.
$gA \frac{\partial h}{\partial x} = -gA \frac{\partial z_b}{\partial x} - g \frac{Q Q }{C^2 R_h A}$	Diffusive wave: Acceleration and inertial terms are neglected, but variation of water depth (pressure term) is allowed. Diffusive models backwater effects. The wave attenuates and there is hysteresis.
$\frac{\partial}{\partial x} \left(\frac{Q^2}{A} \right) + gA \frac{\partial h}{\partial x} = -gA \frac{\partial z_b}{\partial x} - g \frac{Q Q }{C^2 R_h A}$	Dynamic, quasi-steady wave: Only acceleration term is neglected.

Table 1. Simplified forms of Equation 1b

The Saint-Venant (or shallow water) equation forms a system of nonlinear hyperbolic partial differential equations. The hyperbolicity implies that the set of two nonlinear partial differential equations in Equation 1 can be transformed into a set of four ordinary differential equations,

$$\frac{D}{Dt}(V + 2c) = \left[\frac{\partial}{\partial t} + (V + c) \frac{\partial}{\partial x} \right] (V + 2c) = -gA \frac{\partial z_b}{\partial x} - g \frac{Q|Q|}{C^2 R_h A} \quad (2a)$$

$$\frac{D}{Dt}(V - 2c) = \left[\frac{\partial}{\partial t} + (V - c) \frac{\partial}{\partial x} \right] (V - 2c) = -gA \frac{\partial z_b}{\partial x} - g \frac{Q|Q|}{C^2 R_h A} \quad (2b)$$

$$\frac{dx}{dt} = V + c = V + \sqrt{gA/B} \quad (\text{denoted as } C^+ \text{ characteristic line or 2-characteristics}) \quad (2c)$$

$$\frac{dx}{dt} = V - c = V - \sqrt{gA/B} \quad (\text{denoted as } C^- \text{ characteristic line or 1-characteristics}) \quad (2d)$$

where D/Dt is the total derivative, V the average cross sectional velocity, and $c = \sqrt{gA/B}$ is the celerity of the small gravity waves on the surface. In the case of a rectangular prismatic channel, the expression for the celerity of surface gravity waves reduces to $c = \sqrt{gh}$.

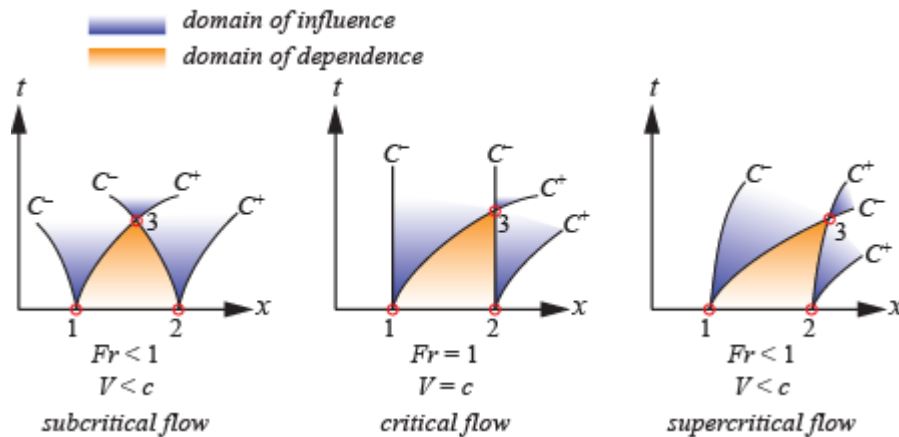


Figure 3. Families of characteristic lines for different flow regimes

Equation 2a is valid along the characteristic line defined by Equation 2c, and Equation 2b is valid along the characteristic line defined by Equation 2d. The characteristic lines define two families of curved lines in the space time domain $x-t$ along which perturbations travel.

Perturbation created at any location along a channel travels along the two characteristic lines emanating from that location. Figure 3 shows the families of C^+ and C^- characteristic lines for different flow regimes. The region between two characteristic lines emanating from a given point

is the domain of influence of that point. The C^+ emanating from point 1 and C^- emanating from point 2 intersect at point 3. The region defined by points 1, 2, and 3 is the domain of influence of point 3. In a subcritical regime, the perturbations travel upstream and downstream. When flow becomes critical, C^- lines become vertical and the perturbations can no longer travel upstream. In supercritical flow, both characteristics carry the perturbations downstream. As demonstrated later in this paper, the direction of travel of perturbations is crucial in designing numerical schemes that can simulate mixed flow regimes.

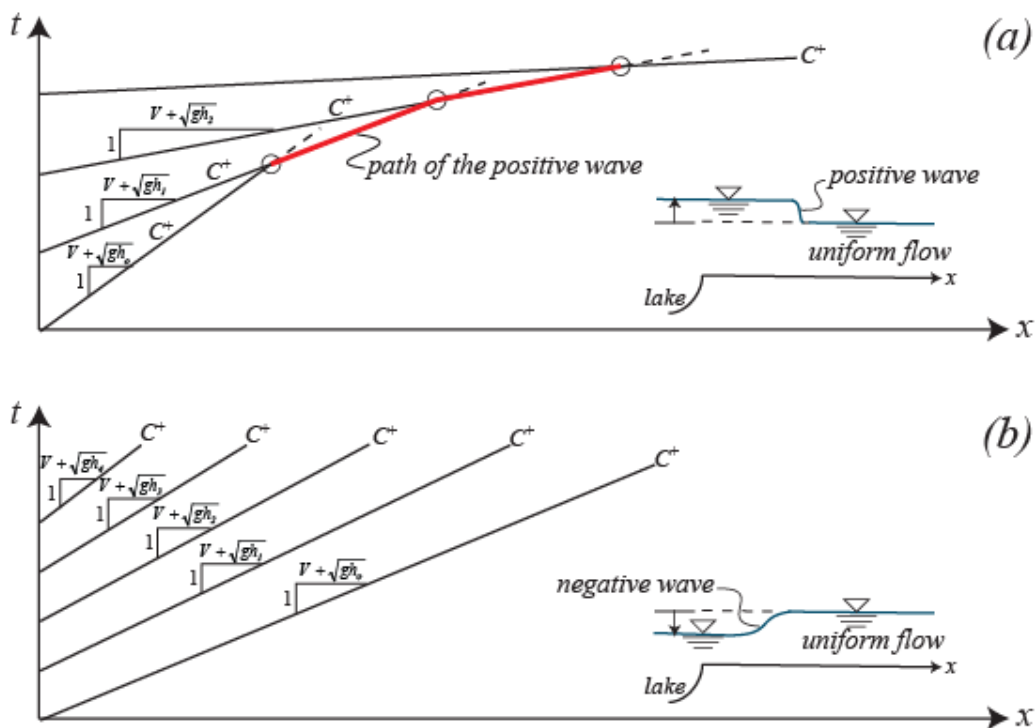


Figure 4. Explaining positive and negative waves using characteristic lines

The method of characteristics can be used to explain the two basic wave types (i.e., positive and negative waves or surges). Referring to Figure 4, consider a long rectangular channel carrying water from a lake with a uniform flow of depth h_0 and velocity V . The upstream end of the

channel terminates in a lake; for the sake of simplicity, neglect the friction forces. Thus, the C^+ and C^- characteristics become straight lines. Consider first the case shown in Figure 4a, where the water surface in the lake is rising rapidly. As the depth increases, the celerity of gravity surface waves issued at the upstream end of the channel increases. The C^+ lines carrying information regarding depth increase are shown with decreasing slopes. Faster traveling new lines catch up with slower traveling older lines, leading to a steep wave front, known as a positive wave. In Figure 4b, the water surface in the lake is rapidly lowered. As the depth decreases, the celerity of gravity surface waves issued at the upstream end of the channel decreases. This results in a series of diverging C^+ lines corresponding to a negative wave. Negative waves are dispersive, and tend to stretch and become less and less pronounced, whereas positive waves tend to keep a steep front.

Referring to Figure 5, consider dam break wave on a horizontal rectangular channel. The height of the dam, originally located at $x = 0$, is h_D and the downstream channel is dry, i.e., $h_t = 0$. The break of the dam generates a negative wave. The downstream tip of the negative wave travels downstream with a celerity of $2\sqrt{gh_D}$ whereas the upstream tip of the negative wave travels upstream with a celerity of $\sqrt{gh_D}$. The initial dam and the shape of the negative wave at intermediate times are shown in Figure 5. It is interesting to note that the negative wave pivots around a point located at a height of $h = (4/9)h_D$. The divergent characteristic lines corresponding to the negative wave are shown at the bottom of the figure. The characteristic line corresponding to $h = (4/9)h_D$ is a vertical line located at the initial dam location. Considering that initial velocities are null, the following relationships can be given (Graf and Altinakar, 2002):

Celerity for any depth: $c_t(h) = -3\sqrt{gh} + 2\sqrt{gh_D}$ (3)

Velocity at any depth: $V(h) = -2\sqrt{gh} + 2\sqrt{gh_D}$ (4)

Negative wave profile at any time: $x = c_t t = (-3\sqrt{gh} + 2\sqrt{gh_D})t$ (5)

The velocity at the point $x = 0$ remains constant and equal to:

$$V_{x=0} = \frac{2}{3}\sqrt{gh_D}$$
 (6)

The unit discharge (i.e., the discharge per unit width) due to the dam break is therefore:

$$q = \frac{8}{27} h_D \sqrt{gh_D}$$
 (7)

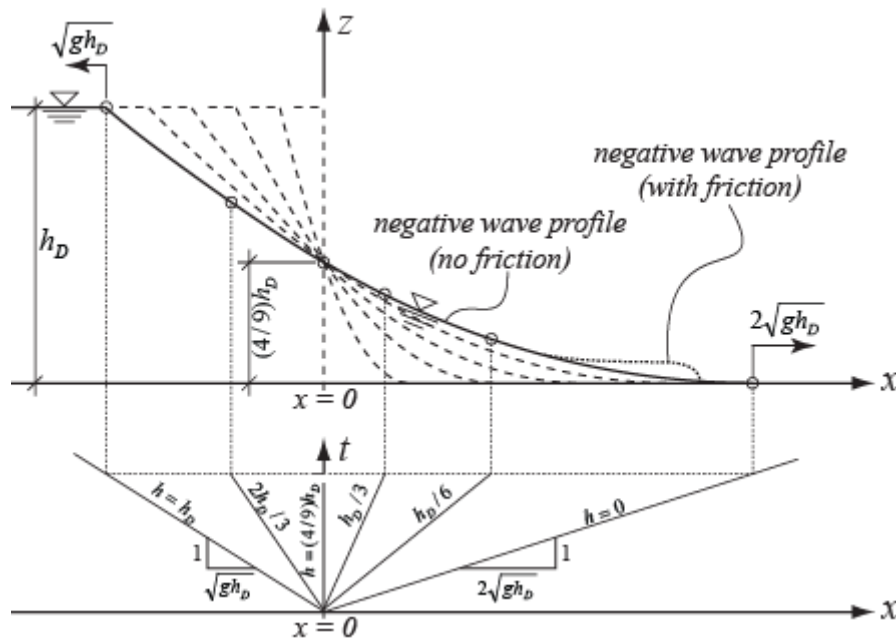


Figure 5. Ideal dam break wave in a frictionless dry, horizontal channel with rectangular cross-section

The foregoing discussion considered the ideal case of a dam-break wave on a dry and frictionless downstream channel. In this case, the negative wave profiles remain self-similar (Ritter, 1982). When friction is introduced, the tip of the negative wave becomes a positive wave and the celerity is reduced. More information on the influence of friction and dam-break in a sloping channel can be found in Chanson (2004). Leal et al. (2006) discusses the dam-break wave-front celerity with and without sediment transport.

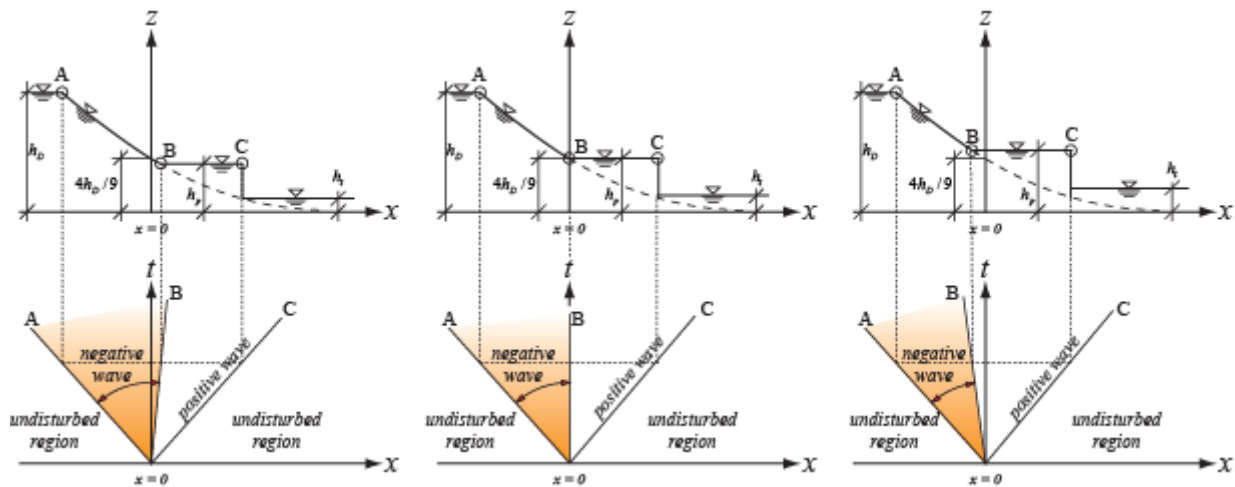


Figure 6. Dam-break flow types and the associated wave structures for different downstream depths

Figure 6 shows the dam-break flow and associated wave structure in the $x-t$ plane when the downstream channel has stagnant water of depth h_t . As shown above, the left and right undisturbed regions are separated by a negative wave (also called a rarefaction wave) on the left and a positive wave on the right. The solution for the negative wave was provided in equations 3-5. The method for finding the height and celerity of the positive wave can be found in Graf and Altinakar (2002). It is important to note that in the leftmost figure, the downstream water depth is

small and the positive wave height is less than $4h_D/9$. Point B travels downstream. In the case of the center figure, the downstream water depth is slightly higher, making the positive wave height equal to $4h_D/9$. The characteristic line for point B becomes vertical, meaning that point B remains at $x = 0$. Finally, in the rightmost figure, the downstream depth leads to a positive wave height greater than $4h_D/9$, which makes point B travel upstream. The importance of these basic wave structures in developing Godunov-type shock capturing upwind schemes is shown in a later section of this paper.

NUMERICAL SOLUTION OF SHALLOW WATER EQUATIONS

The shallow-water (Saint-Venant) equations, Equation 1, which govern the unsteady free surface flows in open channels, form a system of nonlinear hyperbolic partial differential equations. Analytical solution of these equations is only available for a few simplified cases. Real-life engineering problems involving irregular channel cross-sections (or irregular topography for 2D problems) and complex boundary conditions can only be solved using numerical methods. Generally, three classical discretization methods are used for the numerical solution of Equation 1: finite difference method, finite volume method, and finite element method.

Moreover, the solution can be obtained using an implicit or explicit scheme. In the explicit scheme, values at the next time step are computed solely based on the known values of the variables at the current time step. This method is quite straightforward to program, and does not involve solving large systems of equations. The disadvantage of the explicit method is that it generally requires small time steps to ensure stability. Given a grid size, the time step must be chosen to ensure that the fastest wave cannot propagate a distance longer than the smallest grid

size during a single time step. This is called Courant–Friedrichs-Lewy (CFL) condition for stability of the solution. CFL condition in some cases may lead to very small time steps, thus requiring long computational times.

The implicit method computes the values of variables at the next time step based on both currently known values and future unknown values. This leads to a system of equations that must be solved simultaneously. The implicit methods generally have no restrictions on the time step to ensure the stability of the computations. One can use time steps considerably larger than those used in an explicit scheme. In practice, however, the size of the time step must be restricted due to convergence and accuracy considerations. In 2D models, if the domain is large and the grid resolution is high, implicit methods may lead to the solution of very large systems of equations.

Dam-break flows and flash floods are generally rapidly varying unsteady flows, which are quite different than the slowly varying fluvial floods in rivers. Their numerical solution involves additional challenges:

- Dam-break flows and flash floods generally involve presence of mixed flow regimes (subcritical, transcritical, and supercritical) in the same computational domain. At a given location, the flow may also evolve from one regime into another. Handling of these types of flows requires special considerations with regard to boundary conditions and the computational algorithms.
- As shown in the previous section, dam-break flows may involve discontinuities in the flow such as positive transitory waves, standing or moving hydraulic jumps, etc. To capture and resolve these discontinuities, special “shock capturing schemes” need to be used based on the

integral formulation of the conservative form of shallow water equations. These shock capturing schemes must be specially designed to avoid smearing of discontinuities and the oscillations near the edges of discontinuities.

- Dam-break flows may involve dry conditions downstream of the dam. Special numerical procedures must be used to handle wet-dry contact in order to accurately compute the propagation of the wave front.
- Large variations in channel bed elevation and cross-section geometry in 1D problems and complex natural topography in 2D problems may lead to large source terms in Equation 1 (the terms on the right-hand side) in some cases. In order to avoid numerical instabilities and preserve the monotonicity and positivity of flow depth, the numerical schemes must be designed to be “well balanced.”

It is important to note that many numerical models currently used in dam break analysis, such as HEC-RAS (HEC, 2008a) and FLDWAV (Fread, 1993), were originally developed for simulating slowly varying unsteady flows in streams, and therefore ignore most of the challenging aspects mentioned above. These models employ a four-point nonlinear implicit finite-difference scheme to solve shallow water equations, which is a special version of the Preissmann (1961) scheme developed by Fread (1985). This scheme uses centered difference and does not take into account the wave structure of the equations. This numerical scheme gives good results when the flow is entirely subcritical or supercritical; however, it becomes unstable when the simulation involves mixed flow regimes. The User’s Manual for HEC-RAS (HEC, 2008b) attributes this instability to the fact that when the flow passes through a critical depth, the derivatives become large and cause oscillations in the solution. In fact, there are also other reasons regarding to the

specification of boundary conditions that makes the Preissmann scheme invalid for transcritical flows. Additional information can be found in Meselhe (1997).

In FLDWAV, difficulties associated with the simulation of transcritical flow are addressed using a special technique that avoids Saint-Venant equations at the point where mixed flow occurs.

The program automatically subdivides the total length of the stream into sub-reaches wherein only subcritical or supercritical flows occur.

In HEC-RAS, stability problems resulting from the presence of mixed flow regimes is avoided by introducing an option called “Local Partial Inertia” (LPI) technique.” This technique was first developed by Fread (1986) for HEC-UNET, which has now become the unsteady solver for HEC-RAS. It consists of modifying the momentum equation by introducing a multiplier, σ , in front of the acceleration and inertia terms on the left side, such as:

$$\sigma \left[\frac{dQ}{dt} + \frac{\partial \beta Q^2 / A}{\partial x} \right] = -gA \left(\frac{\partial Z}{\partial x} + S_f \right) \quad (8)$$

where S_f represents the friction slope and β is the momentum correction coefficient that takes into account non-uniform velocity distribution. The LPI multiplier is defined as a function of the local Froude number:

$$\begin{aligned} \sigma &= F_T - F_r^m & \text{if } F_r \leq F_T; m \geq 1 \\ \sigma &= 0 & \text{if } F_r > F_T \end{aligned} \quad (9)$$

where F_r is the Local Froude number of the flow, and F_T is the Froude number threshold at which σ is set to zero. In HEC-RAS, this value can range from 1.0 to 2.0 (the default is 1.0).

The exponent m controls the shape of the curve for σ as shown in Figure 7. The default value for m is 10. It is important to note that the LPI is a procedure that converts the full-dynamic unsteady momentum equation into a diffusive flow equation (Table 1) by getting rid of the inertia terms, as the Froude number of the flow approaches 1 (critical flow).

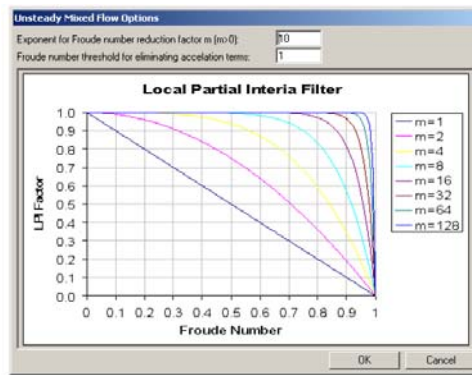


Figure 7. HEC-RAS graphical user interface window to input the parameters for the LPI method (HEC, 2008b)

HEC-RAS and FLDWAV do not contain any considerations regarding the wet-dry fronts, or flow discontinuities. As such, these models may experience instabilities under certain flow situations. In recent years, considerable advances were made in the development of shock-capturing numerical schemes for 1D and 2D applications.

SHOCK-CAPTURING FINITE VOLUME METHODS FOR SOLVING SHALLOW WATER EQUATIONS

An important characteristic of hyperbolic partial differential equations is that even smooth initial conditions may lead to discontinuities (positive waves) propagating at finite speeds. In order to simulate unsteady flows with mixed flow regimes and discontinuities, it is necessary to take into account the wave structure of the shallow water equations. The challenge in developing numerical schemes for solving systems of hyperbolic partial differential equations reside in approximating smooth solution regions with high spatial accuracy while capturing discontinuities as sharply as possible without any oscillations. In the last couple of decades, important advances have been made in this area with the introduction of finite volume high-resolution upwind methods, which take into account the wave structure of the equations and direction of the propagation of the perturbations, and capture the discontinuities sharply without requiring the explicit tracking of wave fronts. Additional techniques are also employed to appropriately handle wet-dry contacts and complex bottom topography..

The shallow water equations given in Equation 1 are not in conservative form. The momentum equation, Equation 1b, involves the spatial derivative of depth, which is not conserved across a flow discontinuity, such as a positive wave or a hydraulic jump. For solving problems with mixed flow regimes and discontinuities, it is preferred to use conservative (or divergence) shallow water equations. The conservative form of shallow water equations can be written in several ways:

$$\frac{\partial A}{\partial t} + \frac{\partial Q}{\partial x} = q_t \quad (10a)$$

$$\frac{\partial Q}{\partial t} + \frac{\partial}{\partial x} \left(\frac{Q^2}{A} + gI_1 \right) = gI_2 - gA \frac{\partial z_b}{\partial x} - g \frac{Q|Q|}{C^2 R_h A} \quad (10b)$$

where I_1 accounts for the hydrostatic pressure force on the wetted cross-section, and I_2 accounts for the pressure forces exerted by the wall in non-prismatic channels. In Equation 10, the term $(Q^2 / A + gI_1)$ is conserved across a flow discontinuity; thus, the equation is in conservative form. In this paper, the following conservative form of shallow water equations is considered:

$$\frac{\partial A}{\partial t} + \frac{\partial Q}{\partial x} = q_t \quad (11a)$$

$$\frac{\partial Q}{\partial t} + \frac{\partial}{\partial x} \left(\frac{Q^2}{A} \right) = -gA \frac{\partial Z}{\partial x} - g \frac{Q|Q|}{C^2 R_h A} \quad (11b)$$

in which $Z = z_b + h$ stands for the water surface elevation with respect to a reference datum.

Equation 11 can be rewritten in vector form as:

$$\frac{\partial \mathbf{U}}{\partial t} + \frac{\partial \mathbf{F}(\mathbf{U})}{\partial x} = \mathbf{S}(\mathbf{U}) \quad (12)$$

where \mathbf{U} is the vector of conserve variables, $\mathbf{F}(\mathbf{U})$ is the flux vector and $\mathbf{S}(\mathbf{U})$ represents forcing function consisting of source and sink terms. These are defined as follows:

$$\mathbf{U} = \begin{bmatrix} A \\ Q \end{bmatrix} ; \quad \mathbf{F}(\mathbf{U}) = \begin{bmatrix} Q \\ \frac{Q^2}{A} \end{bmatrix} ; \quad \mathbf{S}(\mathbf{U}) = \begin{bmatrix} q_t \\ -gA \left(\frac{\partial Z}{\partial x} \right) - g \left(\frac{n^2 Q|Q|}{R^{4/3} A} \right) \end{bmatrix} \quad (13)$$

Equation 12, which is in differential form, can be cast in integral form that accepts discontinuities. Figure 8 shows the solution space $x-t$ discretized by dividing it into cells of size $\Delta x \times \Delta t$. Integrating Equation 10 over the control volume $\Delta x \times \Delta t$ (shaded region in Figure 8) and applying the Green's theorem, the integral form Equation 12 is obtained:

$$U_i^{n+1} = U_i^n - \frac{\Delta t}{\Delta x_i} (F_{i+1/2} - F_{i-1/2}) + \Delta t S_i^n \quad (14)$$

It should be noted that the derivation of Equation 14 (for details see Krishnappan and Altinakar, 2005), which accepts discontinuous solutions, does not involve any approximations. In this

equation, the terms U_i^n and U_i^{n+1} represent the cell averages of conserved variables, located at the cell centers, at the current and future times, respectively. The intercell flux terms $F_{i-1/2}$ and $F_{i+1/2}$ represent the time integrals of the fluxes at the left and right boundaries, respectively. Finally, the term S_i^n accounts for the source and sink terms integrated over the computational cell.

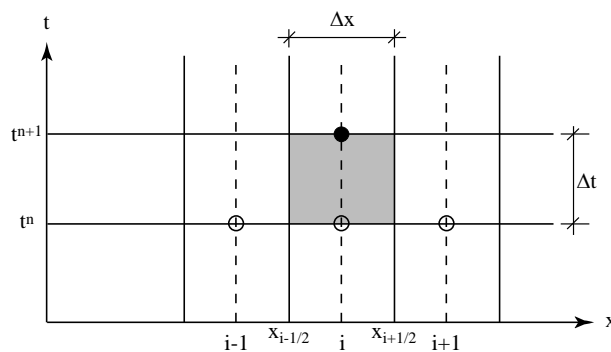


Figure 8. Discretization of the solution domain for solving 1D shallow water equations

Equation 14 can be directly used to evolve the solution from a set of known initial values. It can thus be used as the starting point to develop various types of finite volume schemes. The crucial point is the way the flux terms are written. According to the CFL condition, the maximum distance that a perturbation can travel during the time step Δt is given by $(V + c) \Delta t$. If the time step is kept sufficiently small to satisfy the inequality $(V + c) \Delta t < \Delta x$, the intercell flux terms, $F_{i-1/2}$ and $F_{i+1/2}$, can be expressed in terms of the F values of the conserved variables at the cell centers on each side of the interface.

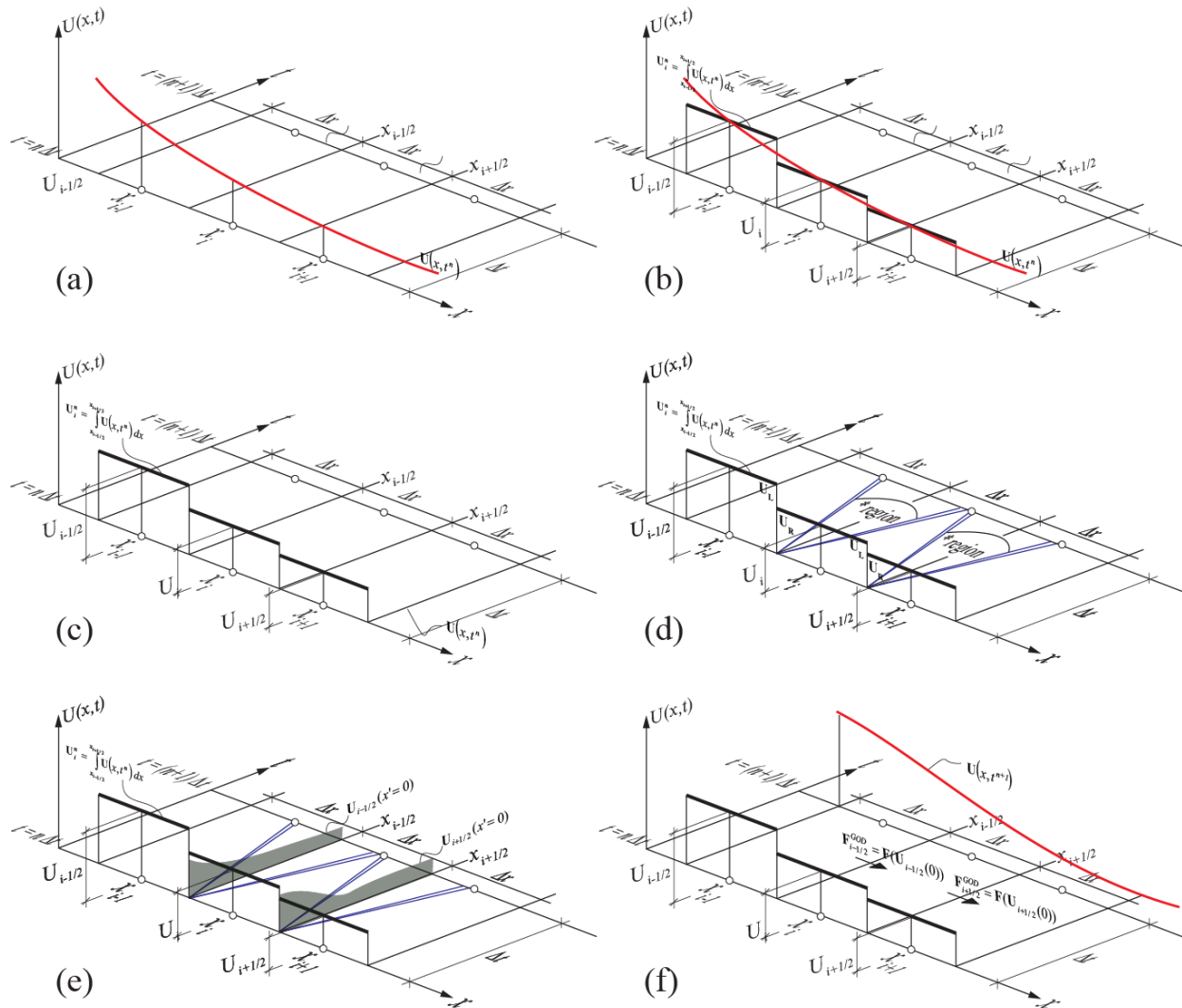


Figure 9. Computational procedure for 1st order Godunov type upwind scheme

In a number of classical schemes, the intercell fluxes are expressed without considering the wave structure of the equation. The most popular schemes include the Forward Time Centered Space, Lax-Friedrichs, and Godunov Centered. On the other hand, Godunov type upwind methods aim to write the intercell fluxes by taking into account the wave structure of the equations to achieve a better representation of the propagation of information in the computational domain. This is

achieved by solving the generalized Riemann problem at each interface to find the value of the intercell fluxes. The general idea behind Godunov type upwind schemes is depicted in Figure 9.

a) Consider a 1D problem along the x axis. The horizontal plane represents the $x - t$ solution domain. The vertical axis corresponds to conserved variables. The channel along the x axis discretized using a cell size of Δx . A time step of Δt is chosen respecting the CFL condition. At time $t = n \Delta t$ the solution vector $\mathbf{U}(x, t^n)$ is known everywhere along the x axis (initial condition). The aim is to evolve this initial solution to find the solution at time $t = (n + 1) \Delta t$ by respecting the wave structure and the propagation direction of the information.

b) First, the cell averages are calculated by integrating the initial values:

$$\mathbf{U}_i^n = \int_{x_{i-1/2}}^{x_{i+1/2}} \mathbf{U}(x, t^n) dx \quad (15)$$

These cell averages are attributed to the cell centers.

c) The initial solution is represented as a piecewise constant function with discontinuities at cell interfaces.

d) In order to properly take into account the propagation of information, each cell interface will include the *Generalized Riemann Problem* (GPR) formula, which is defined as follows:

$$\frac{\partial \mathbf{U}}{\partial t} + \frac{\partial \mathbf{F}(\mathbf{U})}{\partial x} = \mathbf{S}(\mathbf{U}) \quad \text{with} \quad \mathbf{U}(x', 0) = \begin{cases} \mathbf{U}_L(x') & \text{if } x' < 0 \\ \mathbf{U}_R(x') & \text{if } x' > 0 \end{cases} \quad (16)$$

In the classic dam-break problem, the water upstream and downstream of the dam have zero velocities. As shown in Figure 10, the GPR is a generalized form of the dam-break problem where the water on both sides of the discontinuity may also have non-zero velocities. The left and right moving waves can be either shock or negative. Four possible wave combinations

are shown at the bottom of Figure 10. As it is evident from the definition given by Equation 16, the GPR is solved in local coordinates (x') centered at the interface.

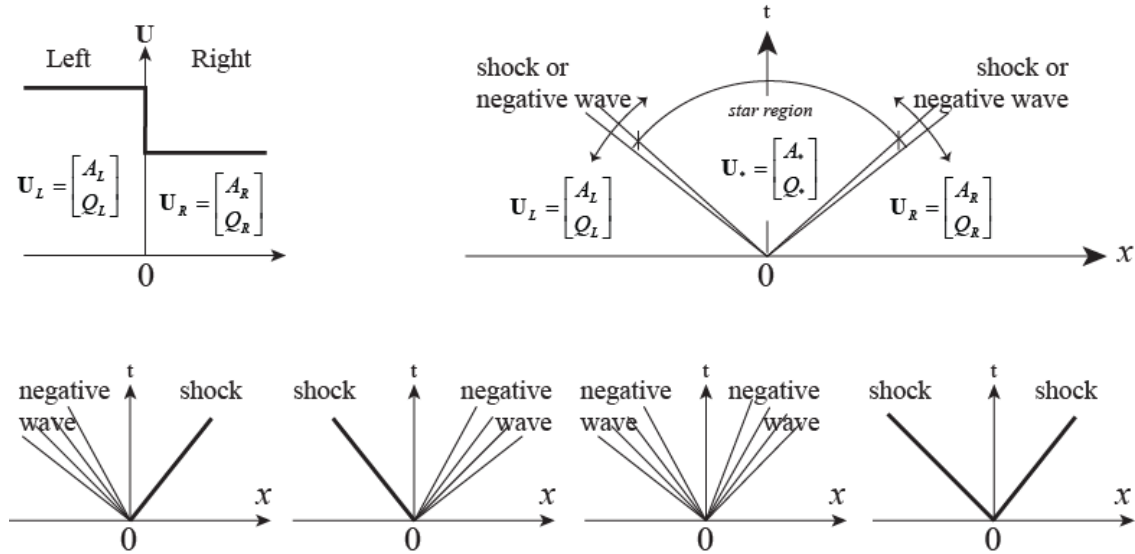


Figure 10. Generalized Riemann Problem (GPR) and the possible wave configurations.

- e) The GPR is solved by either using the exact or an approximate method to find the variation of the variables along the time axis, i.e. $x'=0$. The details of the solution of GPR can be found in Toro (1999 and 2001) and LeVeque (1999 and 2002). Only the variation of conserved variables along $x'=0$, i.e. $\mathbf{U}_{i-1/2}(x'=0)$ and $\mathbf{U}_{i+1/2}(x'=0)$ is needed to construct the Godunov intercell fluxes defined as:

$$\mathbf{F}_{i-1/2}^{GOD} = \mathbf{F}(\mathbf{U}_{i-1/2}(x'=0)) \quad \text{and} \quad \mathbf{F}_{i+1/2}^{GOD} = \mathbf{F}(\mathbf{U}_{i+1/2}(x'=0)) \quad (17)$$

- f) Having determined the intercell fluxes, the solution can be evolved using Equation 14.

This first order Godunov method, which uses piecewise constant representation of initial data, serves as the starting point for a large number of higher order schemes with better accuracy and

less dissipation, such as the Monotone Upstream-centered Schemes for Conservation Laws, Harten, Lax, and van Leer, Weighted Average Flux, etc. Details on these particular schemes can be found in various publications and text books such as Toro (1999 and 2001) and LeVeque (1999 and 2002).

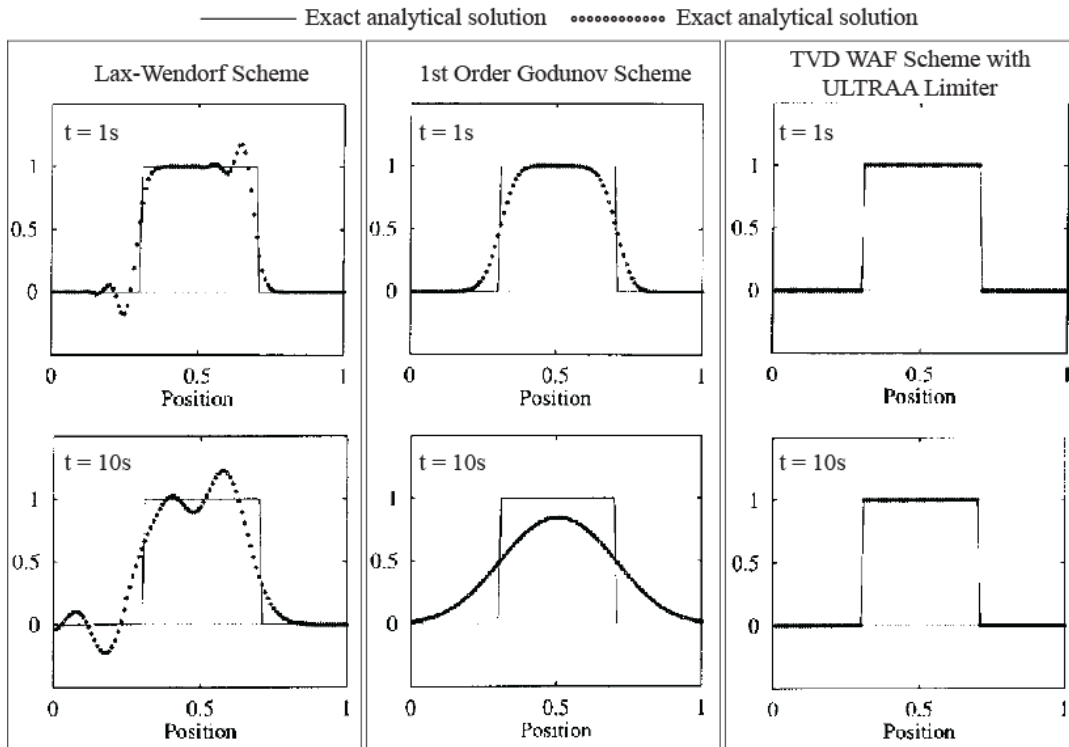


Figure 11. Comparison of numerical solution of the simple advection equation using three different methods

The advantages of modern high-resolution shock capturing methods are depicted in Figure 11, which compares the results of the solution of simple advection equation, $\partial U / \partial t + a (\partial U / \partial x) = 0$ where a is constant, using three different numerical methods. The analytical solution of this problem is shown as $U(x,t) = G(x - at)$, where G is any defined function that may be

discontinuous. In other words, the initial data propagates at constant speed a without changing its shape. Therefore, this simple function is quite helpful in evaluating performance of numerical schemes. In Figure 11, the initial data is a square wave. The solution with the classical Lax-Wendroff scheme, which is second-order accurate in both space and time, shows oscillations near the discontinuities already at $t = 1s$ and at $t = 10s$, is completely deformed. The 1st order Godunov method approximates the square shape at $t = 1s$ with rounded corners; however, due to excessive dissipation, the square shape is completely lost at $t = 10s$. The Total Variation Diminishing (TVD) version of the WAF scheme with ULTRAA slope limiter, is a higher order upwind method that preserves the initial shape of the data even at $t = 10s$.

Shock capturing upwind numerical methods can also be constructed for 2D problems. The next section presents GIS-based decision support system for dam/levee break breaching based on the 2D-simulation of shallow water equations using a shock capturing upwind method.

DSS-WISE INTEGRATED SIMULATION AND CONSEQUENCE ANALYSIS SYSTEM

Figure 12 demonstrates the risk assessment framework for dam safety, as adapted from Bowles (1998) together with the associated modeling tools and/or needs. The DSS-WISE Integrated Simulation and Consequence Analysis System was designed with this framework in mind. It comprises a state-of-the-art 2D numerical model, CCHE2D-FLOOD, for simulating the propagation of a flood discharge resulting from a failure or non-failure event over complex topography, and DSS-WISE, a GIS-based decision support system that can evaluate the consequences of the flood event by interfacing the numerical results with geo-spatial socio-economic data.

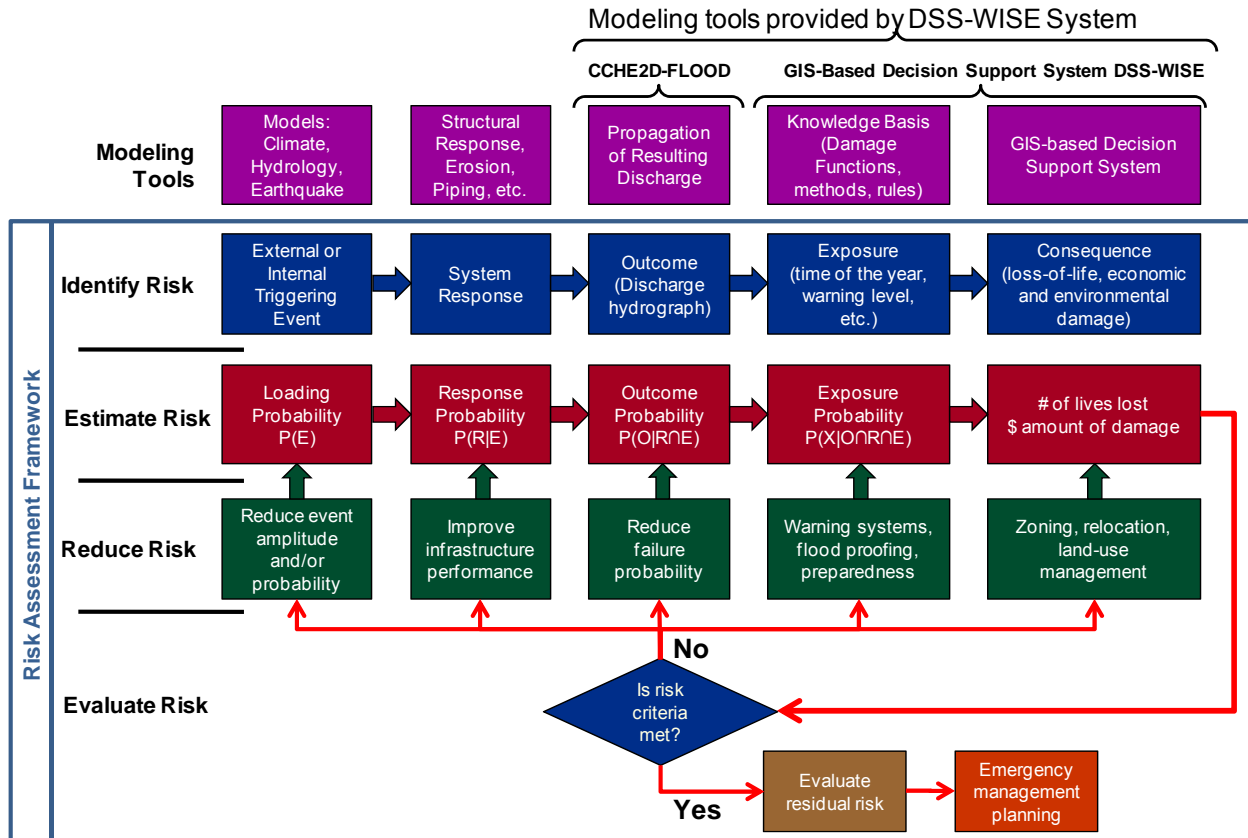


Figure 12. Risk assessment framework for dam-safety and associated modeling tools (adapted from Bowles et al., 1998)

The DSS-WISE System does not provide either the modeling tools for simulating triggering events (i.e., excessive rainfall, earthquake), or modeling tools for computing the structural response of the dam and its appurtenances to these triggering events (i.e., erosion, piping, slope instability, breaching, etc). Simulation of the triggering events and the structural response must be provided by third party tools and methods.

The input to the CCHE2D-FLOOD model can be a discharge entering the reservoir at the upstream end and the evolution of the breach geometry as a function of time, if failure occurs. Since the entire reservoir can be represented as a body of water in the numerical model, the overtopping discharge, in case of non-failure, or the discharge through the breach in case of partial or complete failure will be automatically calculated by the model as the simulation progresses. However, if the bathymetry is not available and the reservoir cannot be represented as part of the 2D solution domain, the hydrograph of the flood at the dam, computed using a third party model, can be directly provided as input for the model. In the following section, the components of the DSS-WISE System are briefly presented and some application examples are given.

CCHE2D-FLOOD Model

The conservative for of 2D shallow water equations in the horizontal plane are given as:

$$\frac{\partial h}{\partial t} + \frac{\partial uh}{\partial x} + \frac{\partial vh}{\partial y} = q_v \quad (18a)$$

$$\frac{\partial hu}{\partial t} + \frac{\partial u^2 h}{\partial x} + \frac{\partial uvh}{\partial y} = -gh(\partial Z / \partial x) - g\left(u\sqrt{u^2 + v^2} / C^2\right) \quad (18b)$$

$$\frac{\partial hv}{\partial t} + \frac{\partial uvh}{\partial x} + \frac{\partial v^2 h}{\partial y} = -gh(\partial Z / \partial y) - g\left(v\sqrt{u^2 + v^2} / C^2\right) \quad (18c)$$

where h is the local flow depth, u and v are local velocities in x and y directions, q_v is a volume source or sink per unit area per unit time, g is gravitational acceleration, and C represents the Chezy coefficient of roughness. The water surface elevation is defined as $Z = z_b + h$ with z_b representing the elevation of the terrain with respect to a reference datum. Equation 18a

represents the conservation of mass, whereas equations 18b and 18c represent the conservation of momentum in x and y directions, respectively.

The above equations are written in conservative (or divergence) form. This refers to the fact that on the left side of Equation 18, the terms with spatial derivatives are conserved across a discontinuity. Therefore, these equations can be used to develop a numerical scheme that accepts flow discontinuities, such as hydraulic jumps, and traveling positive waves. Equation 18 can be cast in vector form follows:

$$\frac{\partial \mathbf{U}}{\partial t} + \frac{\partial \mathbf{F}}{\partial x} + \frac{\partial \mathbf{G}}{\partial y} = \mathbf{S} \quad (19)$$

The vector of conserved variables, \mathbf{U} , the vector of intercell fluxes in x and y directions, $\mathbf{F}(\mathbf{U})$ and $\mathbf{G}(\mathbf{U})$, respectively, and the vector of source and sink terms, $\mathbf{S}(\mathbf{U})$, are defined as follows:

$$\mathbf{U} = \begin{bmatrix} h \\ Q_x \\ Q_y \end{bmatrix} \quad \mathbf{F} = \begin{bmatrix} Q_x \\ Q_x^2/h \\ Q_x Q_y/h \end{bmatrix} \quad \mathbf{G} = \begin{bmatrix} Q_y \\ Q_y Q_x/h \\ Q_y^2/h \end{bmatrix} \quad \mathbf{S} = \begin{bmatrix} 0 \\ -gh(\partial Z/\partial x) - g\left(u\sqrt{u^2+v^2}/C^2\right) \\ -gh(\partial Z/\partial y) - g\left(v\sqrt{u^2+v^2}/C^2\right) \end{bmatrix} \quad (20)$$

Referring to the Cartesian regular computational mesh shown in Figure 1, the finite volume discretization of Equation 19 is obtained by integrating it over a computational cell of $\Delta x \times \Delta y$, and taking the time step to be Δt :

$$U_{ij}^{n+1} = U_{ij}^n - \left(\frac{\Delta t}{\Delta x}\right) (F_{i+1/2,j} - F_{i-1/2,j}) - \left(\frac{\Delta t}{\Delta y}\right) (G_{i,j+1/2} - G_{i,j-1/2}) + \Delta t S_{ij} \quad (21)$$

As shown in the previous section, various formulations can be used to express intercell fluxes. In the case of CCHE2D-FLOOD, a first order upwind flux was implemented (Ying, 2004):

$$\mathbf{F}_{i+1/2,j} = \begin{bmatrix} Q_x \\ Q_x^2/h \\ Q_x Q_y/h \end{bmatrix}_{i+k} \quad k = \begin{cases} 0 & Q_x \geq 0 \\ 1 & Q_x \leq 0 \end{cases} \quad \mathbf{G}_{i,j+1/2} = \begin{bmatrix} Q_y \\ Q_y Q_x/h \\ Q_y^2/h \end{bmatrix}_{j+m} \quad n = \begin{cases} 0 & Q_y \geq 0 \\ 1 & Q_y \leq 0 \end{cases} \quad (22)$$

The source terms are discretized as follows:

$$\mathbf{S} = \begin{bmatrix} q_v \\ -gh_{ij}^{n+1} [(\partial Z / \partial x)] - g \left(u_{ij} \sqrt{u_{ij}^2 + v_{ij}^2} / (h_{ij}^{1/6} / n)^2 \right) \\ -gh_{ij}^{n+1} [(\partial Z / \partial y)] - g \left(v_{ij} \sqrt{u_{ij}^2 + v_{ij}^2} / (h_{ij}^{1/6} / n)^2 \right) \end{bmatrix} \quad \text{with} \quad C = \frac{h_{ij}^{1/6}}{n} \quad (23)$$

where n represents Manning's roughness coefficient. To achieve a well balanced scheme, the water surface gradient is calculated using the following formula:

$$\frac{\partial Z}{\partial x} = \begin{cases} Z_{i+1,j} - Z_{i,j} & \text{if } (Q_x)_{i,j} > 0 \text{ and } (Q_x)_{i+1,j} > 0 \\ Z_{i,j} - Z_{i-1,j} & \text{if } (Q_x)_{i,j} < 0 \text{ and } (Q_x)_{i-1,j} < 0 \\ (Z_{i+1,j} - Z_{i-1,j}) / 2 & \text{all other cases} \end{cases} \quad (24)$$

The model handles dry bed condition by maintaining a very small water depth, so as to not cause any noticeable change in the propagation speed of the wet/dry front. When a wet cell and dry cell share a common edge, only mass flux is permitted into the dry cell. Other additional techniques are also implemented to handle numerical problems arising from the stepped discretization of the topography and the water surface. A discussion of these techniques can be found in Frazão et al (2002).

The CCHE2D-FLOOD code uses an explicit scheme to solve the shallow water equations using the stencil shown in Figure 13. It is subjected to the CFL condition for stability and convergence, which states that during a time step, the wave (or a perturbation) should not travel a distance longer than the smallest cell size. Given a mesh size, the CFL condition places an upper bound on the time step as follows:

$$N_{CFL} = \text{Max} \left[\frac{\Delta t}{\Delta x} (|u| + \sqrt{gh}), \frac{\Delta t}{\Delta y} (|v| + \sqrt{gh}) \right] \leq 1 \quad (25)$$

The time step can be either automatically selected by the program based on the consideration of the CFL condition or directly specified by the user.

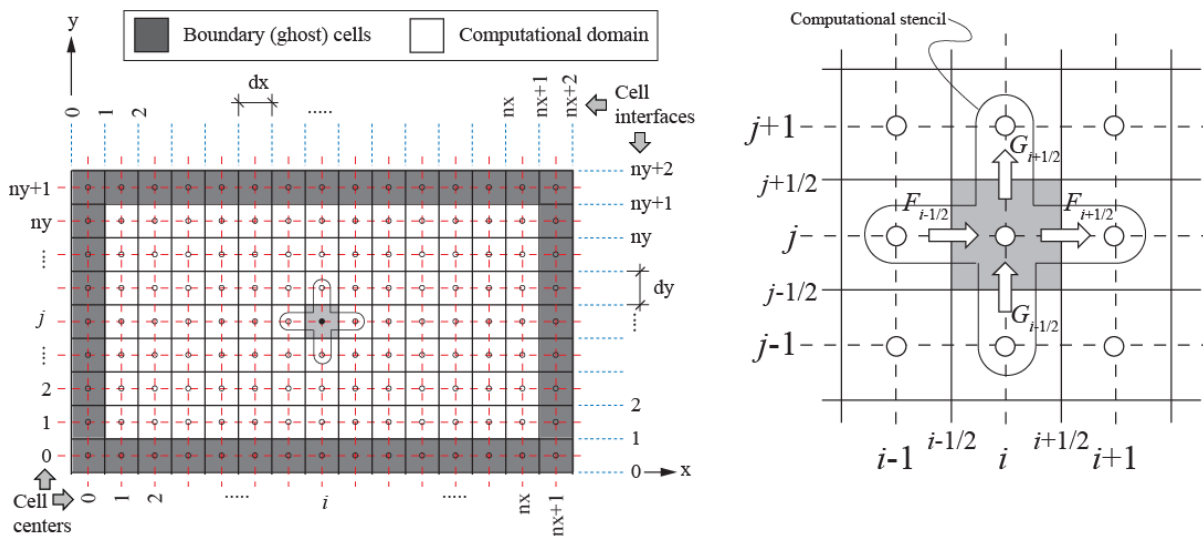


Figure 13. Cartesian computational mesh and the computational stencil used in CCHE2D-FLOOD

The CCHE2D-FLOOD uses a regular Cartesian computational mesh (see Figure 13) representing the topography of the bed, which can be a Digital Elevation Model (DEM) imported from the U.S. Geological Survey Web site or a GIS data clearinghouse. The program automatically defines a single layer of ghost cells around the computational domain. These ghost cells are needed to impose boundary conditions, which can be of type inlet, outlet or fully reflecting wall. Two types of inlet boundary conditions are implemented: time variation of water surface elevation; and incoming discharge hydrograph. Outlet boundaries can have a time varying water surface elevation, discharge as a function of water surface elevation (stage-discharge curve), normal depth boundary, and critical depth boundary.

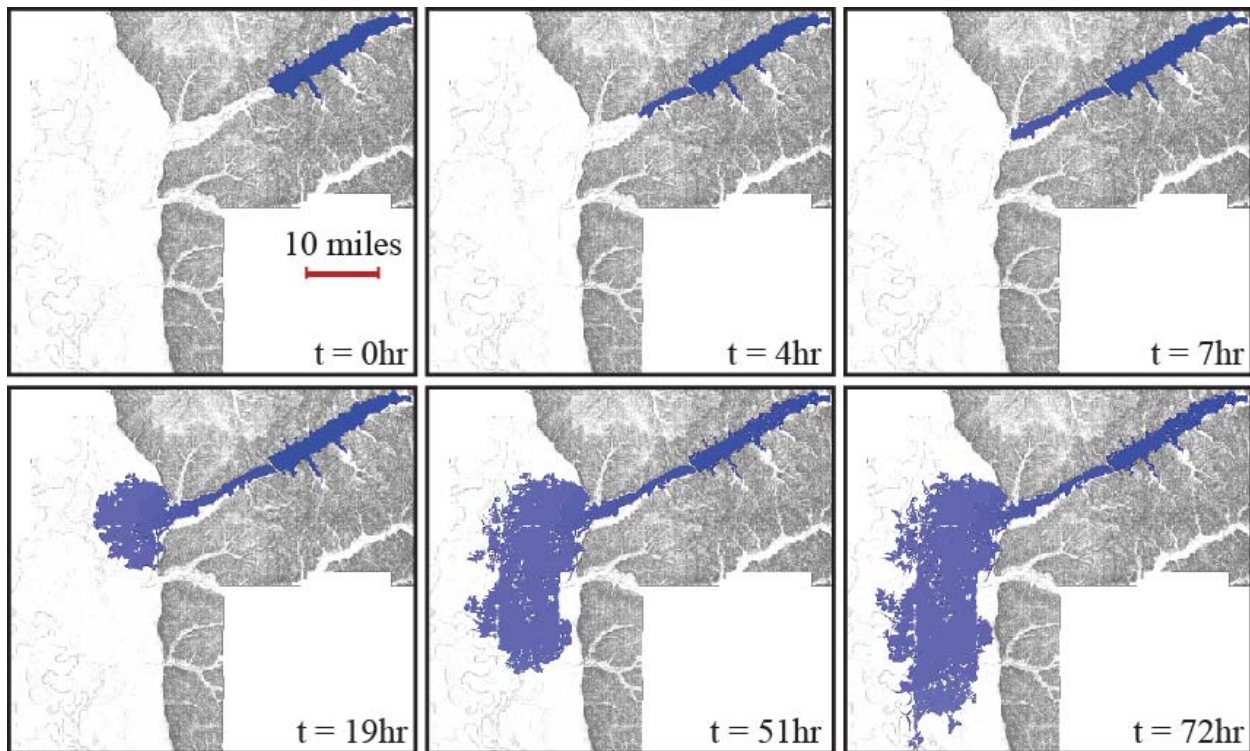


Figure 14. Snapshots of the flood due to a hypothetical sunny-day partial breaching of a dam computed with CCHE2D-FLOOD

CCHE2D-FLOOD was verified using analytical solutions, and validated based on both laboratory test results (see Ying et al., 2003; Ying et al., 2004); the field data from historical dam break cases was obtained from (Ying and Wang, 2004). A preliminary version of CCHE2D-FLOOD has been in use by the U.S. Army Corps of Engineers, Engineer Research and Development Center for dam-break studies. These verification and validation tests and application to several dam-break studies have shown that CCHE2D-FLOOD is robust, stable and conserves mass rigorously. The shocks are captured without any oscillations.

As an example, the CCHE2D-FLOOD was used to simulate a hypothetical sunny-day partial breaching of a dam located in the State of Mississippi. The dam has a crest length of 15,300 feet (4,700 m), and an average height of 97 feet (30 m). At the normal (recreation) pool level, the lake has a surface area of 32,500 acres (132 km²).

The computational domain encompassing the entire lake and the surrounding floodplain is approximately 94 km by 64 km. The cell size is 60m. The hypothetical sunny-day breach scenario assumed the formation of a 200m-wide breach, with side slopes of 25 degrees, in a 30-minute timeframe. The downstream channel was assumed to be dry. The simulation was carried out for 72 hours. Figure 14 shows the snapshots of the flood propagation computed by CCHE2D-FLOOD at different times. During the initial seven hours after breaching, the flood wave is propagating in a relatively narrow valley. The flow can be assumed to be channelized and the one dimensional flow approximations should hold relatively well. During the latter stages, the flood is propagating the flat terrains of the Mississippi Delta, where there is no clear channel definition. As it can be seen from the snapshots in Figure 14, the flood spreads in all directions and the assumptions for 1D flow are violated. It would very difficult, if not impossible, to calculate the flood propagation over the flat terrain using a 1D program. In order to obtain a more accurate estimation of the flood arrival times and the flood delineation, it is necessary to use a 2D program, such as CCHE2D-FLOOD.

Representation of linear terrain features in CCHE2D-FLOOD

Certain terrain features such as road and railroad embankments, levees, and dikes may act as obstacles to the flow and considerably influence the propagation of the flood. These types of terrain features have a small width but continue over long distances. They are referred to as

linear terrain features. Due to their small width, linear terrain features are not always adequately represented in DEMs used for flood studies, which have a typical resolution between 10m to 100m. One alternative is to use a 2D model with unstructured triangular mesh, which allows for the decrease of the mesh size and increase of the mesh density locally to capture linear terrain features in the topography. The disadvantage of this method is that due to the smaller cell size, the time step has to be smaller to guarantee the stability of the numerical simulation. Depending on the type of the problem, this may considerably increase computational time.

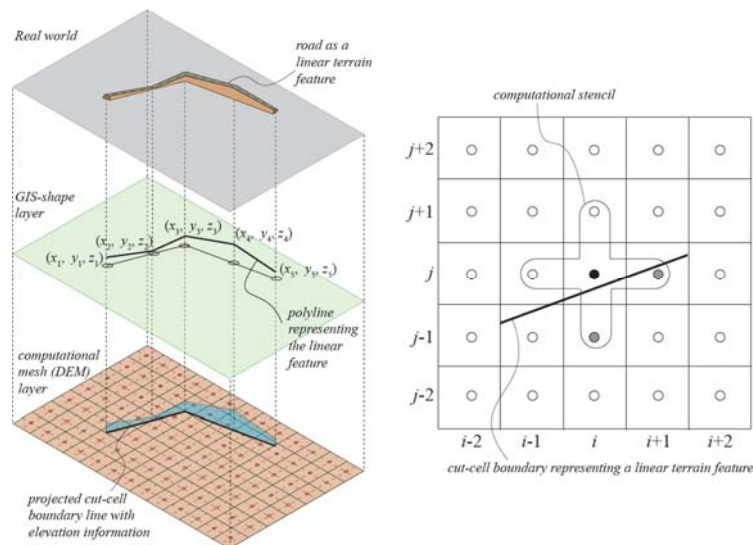


Figure 15 Projection of a linear terrain feature onto the DEM and the incomplete computational stencil for a cell near a cut-cell boundary

CCHE2D-FLOOD gives the user the capability to represent linear terrain features on a regular mesh using a *two-sided cut-cell boundary* capability. In this approach, the linear terrain feature to be represented in the model is projected onto the DEM from a GIS shape layer by imposing that a cell can only be cut by a single straight line (Figure 15). The projected line cuts through some

of the cells of the computational mesh. Computational cells affected by a cut-cell boundary cannot be calculated using the standard computational stencil given by Equation 21. For example, the center cell shaded in black within Figure 15 has an incomplete stencil given that the gray shaded cells are on the other side of the cut-cell boundary. CCHE2D-FLOOD employs a two-sided version of the ghost-fluid method by Ghias et al. (2007). In this method, the first values of the conserved variables in the cell centers that are on the other side of the boundary are replaced by computed values that will enforce the proper boundary computations along the cut-line. The standard stencil is then utilized in a common manner. The net result is that the influence of the cut-cell boundary is included in the computation. This method also allows the user to take into account flows overtopping the linear terrain feature when the flow depth is sufficiently high. The low overtopping cut-cell boundary is calculated using an appropriate weir formula based on the water surface elevations on both sides and the crest elevation of the linear terrain feature. The details of the two-sided cut-cell boundary method are discussed in Miglio et al. (2008), and Altinakar et al. (2009a and 2009b).

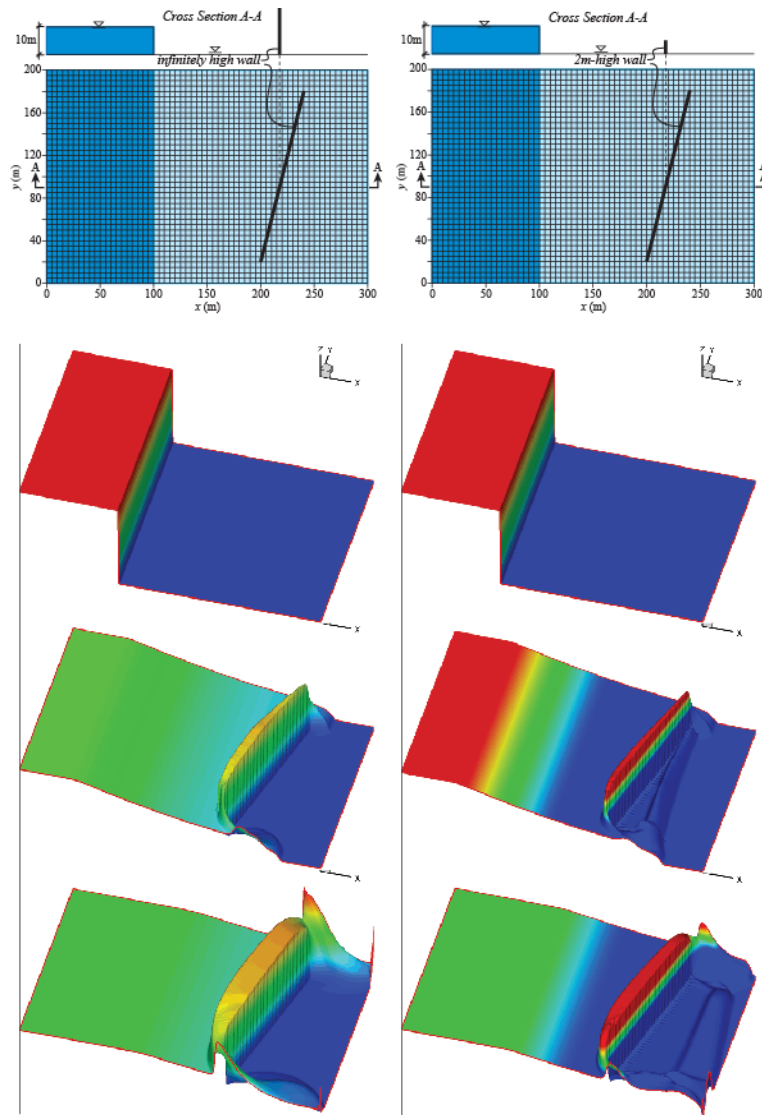


Figure 16. Comparison of the two test cases computed with cut-cell boundary method

Figure 16 compares the results of the two dam-break test cases computed with the cut-cell boundary option representing an oblique wall on an otherwise flat surface. In both cases, breaching of a 10m high dam located on the left side of the domain is simulated. The downstream topography is dry. The oblique wall in the test case on the left is infinitely high, whereas the oblique wall in the test case on the right has a height of 2m; thus, it can be

overtopped. The lower rows compare the instantaneous pictures of the flow field taken at the same time. The second row is the initial situation. In the third row, the tip of the dam-break wave has already hit the oblique wall. On the left, the flow rises behind the wall due to its momentum while some flow goes around the obstacle to the other side. On the right, part of the rising water has spilled downstream and generated a new wave. Finally, the last row on the left water level rising behind the wall has generated a very high positive wave traveling back. On the right, since part of the water has spilled, the water level rise behind the wall is less spectacular and the positive wave has a lower height. The wave generated by the overtopped water is clearly visible.

Coupled 1D-2D simulations using CCHE2D-FLOOD

In CCHE2D-FLOOD, an extension of the cut-cell boundary concept was implemented to provide coupled 1D-2D simulation capability. The river is projected from a GIS-shape layer onto the Cartesian mesh in the same way as a linear terrain feature (see Figure 17). In this particular case, however, the cut-line represents a 1D river model. Therefore, the river cross-sections are also provided along with other data needed to define a 1D river complete with its boundary conditions. In CCHE2D-FLOOD, a 1D river can be defined as a *narrow river* if the width of the river is small compared to the cell size, and as a large river if the river width takes up several cells. In the latter case, the river is defined by two cut-cells defining the left and right bank elevations as two separate cut-cell boundaries. The 2D cells that are covered by the river are blocked and do not participate in the 2D simulation.

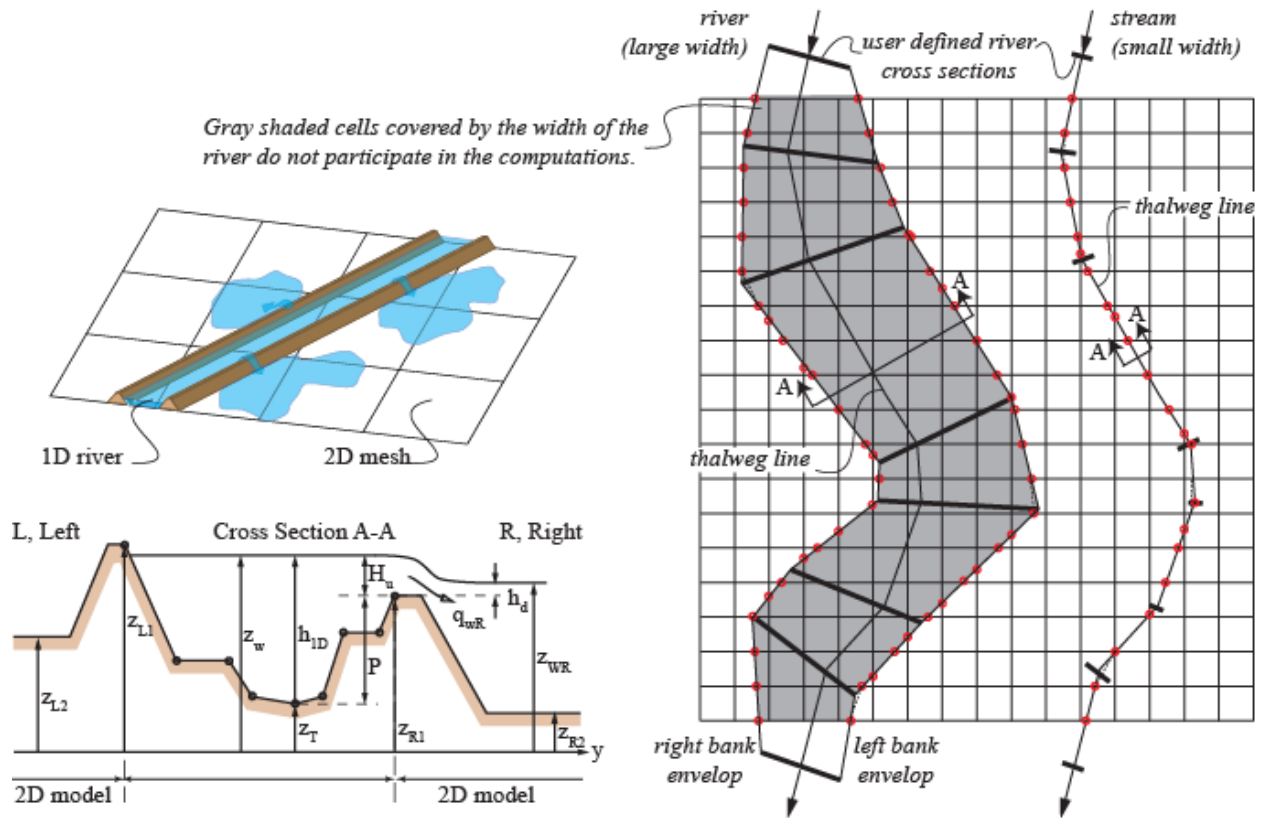


Figure 17. Representation of a 1D river in CCHE2D-FLOOD using cut-cell boundary approach

The discharges exchanged between 1D and 2D models due to overtopping can be in both directions (i.e., from 1D to 2D or vice versa). These exchange discharges are calculated using an appropriate weir equation by taking into account the water surface elevations in the 1D river and the 2D model (left and right exchanges are computed separately). It is important to note that only mass exchange is allowed. There is no momentum exchange between 1D and 2D models. The 1D river model also uses a shock capturing upwind finite-volume method to solve shallow water equations. Details can be found in Altinakar et al. (2009). It handles wetting and drying of cross-sections and mixed flow regimes.

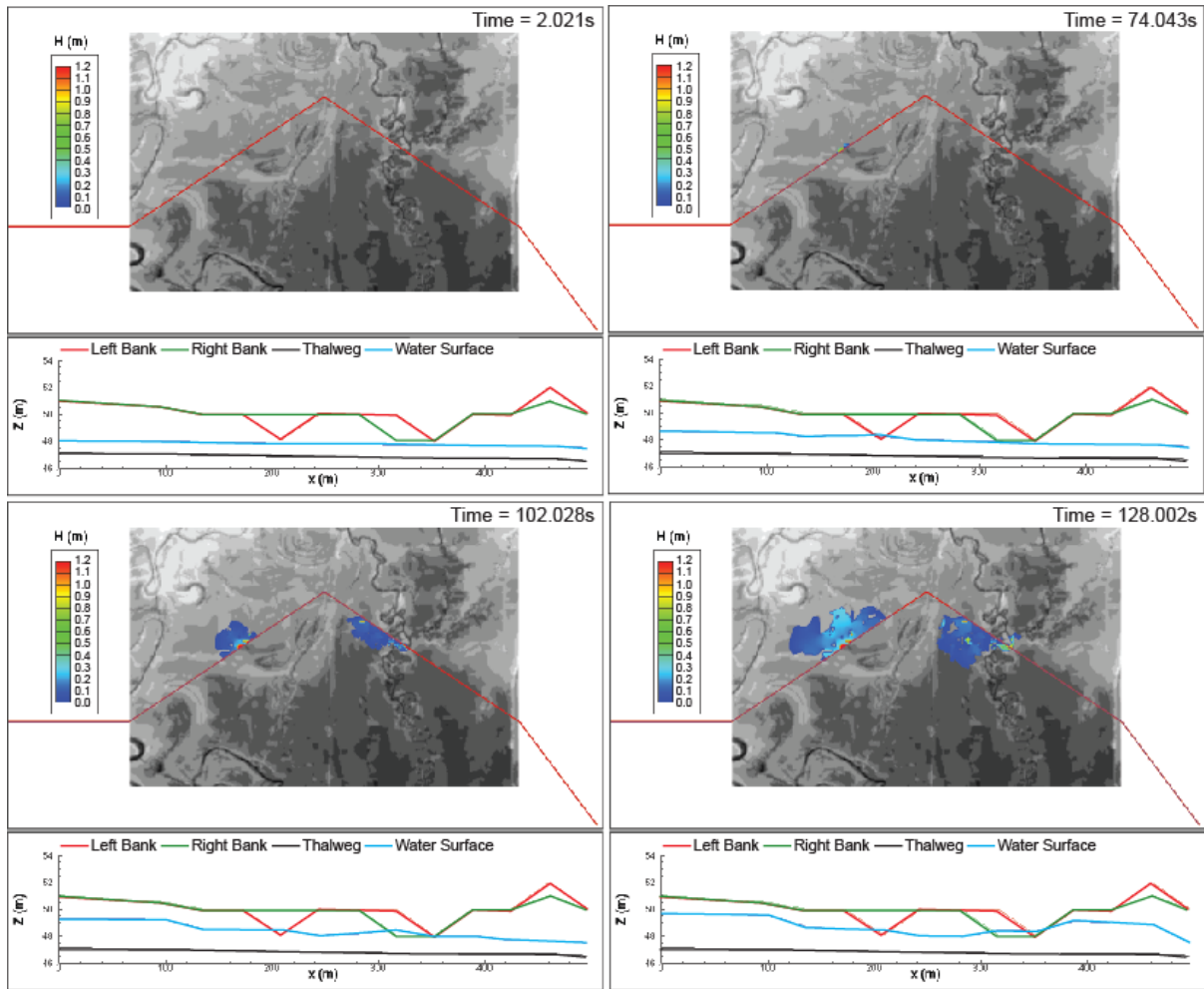


Figure 18. Test case for a coupled 1D-2D computation; taken from Altinakar et al. (2008)

Figure 18 shows a test case of coupled 1D-2D simulation using CCHE2D-FLOOD. The 1D river is modeled as a narrow river using cut-line boundary concept. The flow takes place from left to right. Initially, there is a steady constant discharge flowing in the river. The discharge at the upstream boundary is increased linearly to a maximum value and then decreased back to its initial value. The left bank has low sections located at $x = 210m$ and $x = 350m$, whereas the low section for the right bank is located at $x = 320 - 360m$. As the discharge increases, the water first overtops the low point on the left bank at $x = 210m$. Then, the overtopping from 1D river to 2D

model occurs on the right bank at $x = 320 - 360m$, followed by the overtopping on the left bank at $x = 350m$. The overtopping discharges from the 1D model propagate in the 2D model following the topography. The coupled 1D-2D model option in CCHE2D-FLOOD can be efficiently used to simulate levee overtopping and/or breaching type flows.

GIS-Based Decision Support System DSS-WISE

The DSS-WISE, a GIS-based decision support system, is developed as an extension to the ArcMap 9.3 software developed by ESRI. Figure 19 shows the organization of the DSS-WISE system, which is complementary to CCHE2D-FLOOD. DSS-WISE provides graphical user interface and computational tools for two essential functions: 1) Pre-processing and treatment of available data and preparation of input files for a user defined simulation scenario; and 2) Post-processing tools that interface the results of the numerical flood simulation with geospatial socio-economic data for consequence analysis and mapping.

Overview of Pre-Processing Tools

Although the use of a DEM eliminates the need for mesh generation, it is generally necessary to treat the DEM obtained from a data clearinghouse to clean some unwanted features, to project linear terrain features, and to prepare the input files. The tools described in this section help the user accomplish these tasks.

The Lake Interpolation tool is developed to aid in preparing DEM files to be used as computational mesh for CCHE2D-FLOOD. In general, two principal problems may be encountered. First, the DEM file obtained from a data clearinghouse may contain bodies of water

such as lakes or reservoirs, represented as a flat surface at their free-surface elevation, if the bathymetry is available it can be burned into the DEM. If the bathymetry is not available, the next best option available is its interpolation from the surrounding known topography and estimated point elevations and hand drawn contour lines to be provided by the user. Second, when the dam is represented in the DEM file, it must be removed and replaced with the elevations representing the topography upon breaching. Both of these tasks can be accomplished using the capabilities programmed in Lake Interpolation Tool Box.

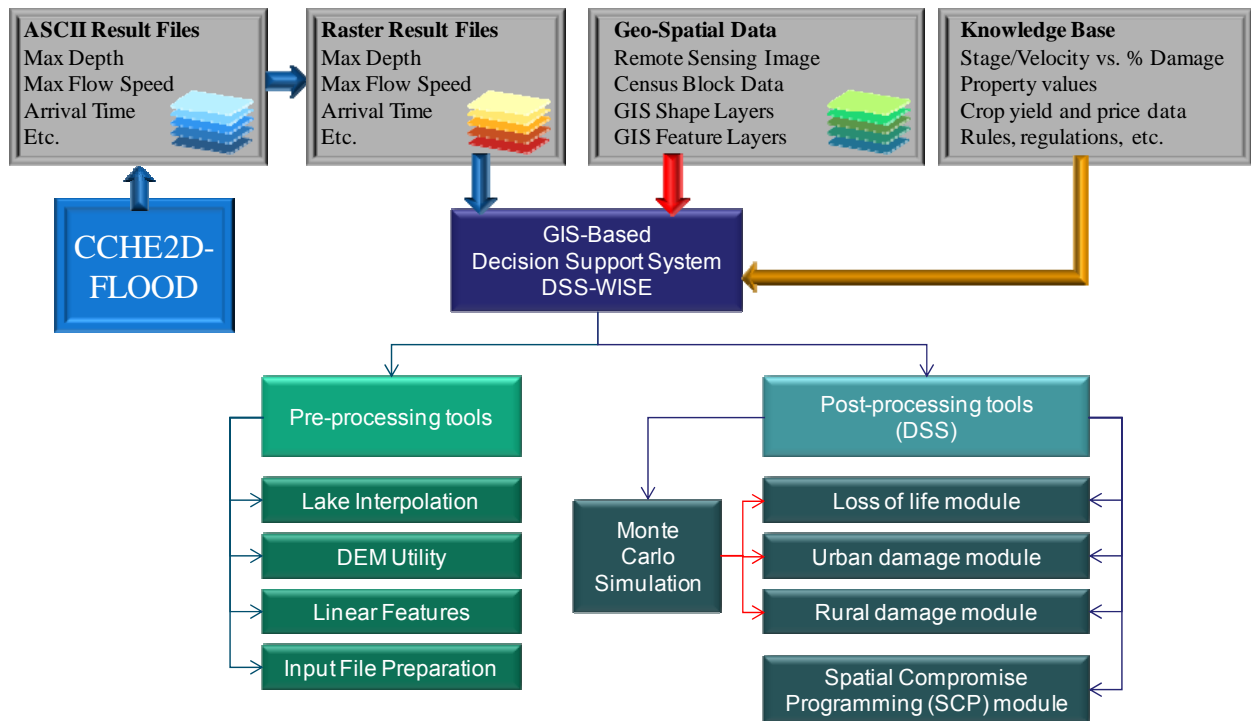


Figure 19. General organization and functionalities of the GIS-based DSS-WISE

The DEM Utility tool allows the user to define the different roughness values for different parts of the DEM based on classified remote sensing images and/or aerial photos.

The linear Features tool is used to project linear terrain features, such as a road or railroad embankment, or a 1D river planview (narrow or wide river), from a GIS shape layer to create the cut-cell boundaries to be used in the computations. The tool helps the user by checking any violation of cut-cell boundary definition rules and helps the user correct them. When the final shape of the cut-cell boundary is consolidated, the Linear Features tool writes all input data files defining cut-cell boundaries automatically.

The input File Preparation tool is used to define the scenario to be solved and to set the parameters of the numerical simulation such as time step, duration of computation, etc. Specific dialog windows help the user to specify locations of dams (there can be multiple dams), their characteristics, breach times, and time evolution of breach geometries. The initial conditions are defined by specifying the locations and water surface elevations of bodies of water (places originally containing still water). The tool automatically fills the lake area using topographic information. Certain areas of the computational domain can be defined as source or sink. The rate of the discharge outgoing from a sink area can be calculated based on the water depth. Controlled release from a reservoir can be simulated using a coupled source and sink definition (outgoing sink discharge is equal to incoming source discharge).

For detailed analyses of results, the user can also define: 1) observation points where the computed variables are stored for further analysis; 2) observation lines for which the discharge crossing the line is recorded; and 3) observation profile along which the results are stored at requested frequency for plotting profiles of water surface elevation, velocity, and discharge, etc.

Overview of Post-Processing Tools

Referring again to Figure 19, CCHE2D-FLOOD provides 2D raster files of 1) flow depths over the entire mesh at prescribed times; 2) velocity components in x and y directions over the entire mesh at prescribed times; 3) maximum depth values for the entire mesh; 4) maximum velocity vectors for the entire mesh; 5) flood arrival time for all cells; and 6) flood duration times for all cells. These raster files can be readily imported into the GIS platform for creating 2D maps by overlaying it with any GIS layers. Using a third party program, the time varying simulation results can also be animated. The post-processing toolbox contains a number of tools to interface results of CCHE2D-FLOOD simulations with various geospatial socio-economic data such as census block information, building stock, and agricultural assets.

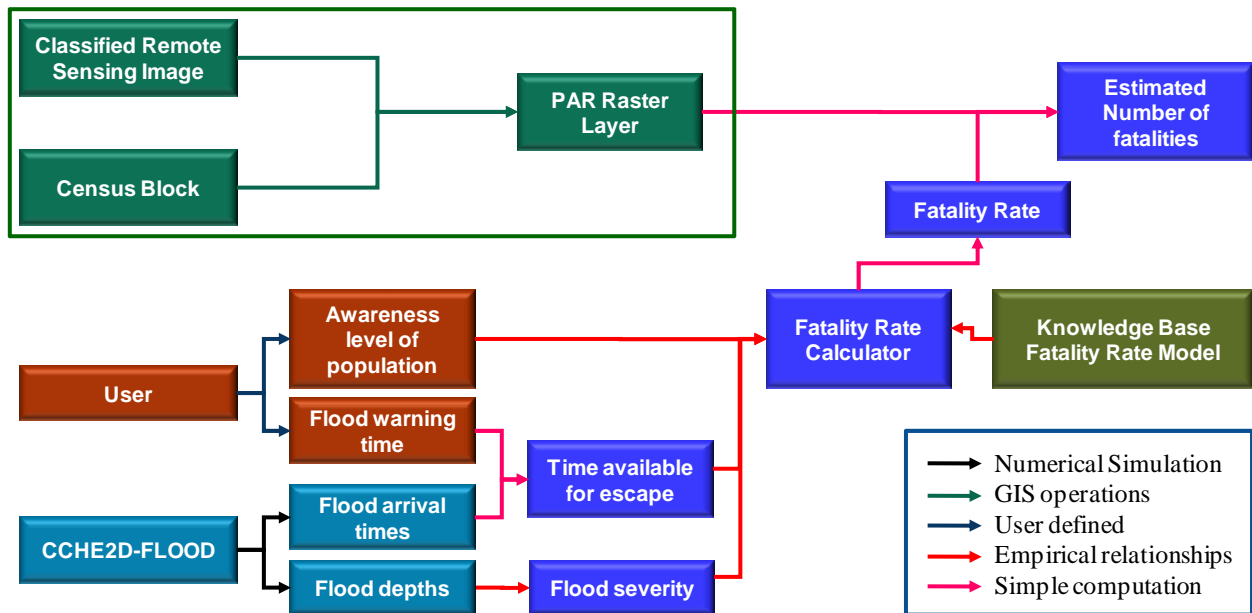


Figure 20. Flow diagram of loss of life method implemented in DSS-WISE

The Loss of life Estimation Tool implements a slightly modified version of the U.S. Bureau of Reclamation procedure developed by Graham (1999). According to this method, loss of life

resulting from flooding depends on three factors: 1) number of people living in the flooded area, identified as population at risk (PAR); 2) amount of warning that is provided to the people exposed to dangerous flooding; and 3) severity level of the flood. The flowchart showing the implementation of this method in DSS-WISE is presented in Figure 20.

Flood Severity	Escape Time	Perception of Flood Severity	Fatality Rate	
			Suggested Range	Value
High ($h_{\max} > 15 \text{ ft}$)	not applicable	not applicable	0.30 – 1.00	0.75
Medium $10 \text{ ft} < h_{\max} < 15 \text{ ft}$	no warning ($T_{esc} < 15 \text{ min}$)	not applicable	0.03 – 0.35	0.15
	some warning $15 \text{ min} < T_{esc} < 60 \text{ min}$	vague	0.01 – 0.08	0.04
		precise	0.005 – 0.04	0.02
	adequate warning $T_{esc} > 60 \text{ min}$	vague	0.005 – 0.06	0.03
precise		0.002 – 0.02	0.01	
Low $h_{\max} < 10 \text{ ft}$	no warning ($T_{esc} < 15 \text{ min}$)	not applicable	0.0 – 0.02	0.01
	some warning $15 \text{ min} < T_{esc} < 60 \text{ min}$	vague	0.0 – 0.015	0.007
		precise	0.0 – 0.004	0.002
	adequate warning $T_{esc} > 60 \text{ min}$	vague	0.0 – 0.0006	0.0003
precise		0.0 – 0.0004	0.0002	

Table 2. Fatality rates for estimating loss of life (adapted from Graham, 1999)

The PAR information is obtained from census block data, which is usually a vector polygon layer (for example, in TIGER format). The classified remote sensing image is used to distribute the population in census block polygons into the cells of a raster image identical to that used in the numerical computation. The information regarding the awareness level of the population and the time at which the flood warning is given is provided by the user. CCHE2D-FLOOD simulation results provide raster images of flood depths and flood arrival time. Referring to Table 2, the flood severity is directly related to the flow depth. Time available for escape for population in each cell, $T_{esc}(x, y)$, is computed from:

$$T_{esc}(x, y) = T_{arr}(x, y) - T_{warn} \quad (26)$$

where $T_{arr}(x, y)$ is the flood arrival time for each cell as computed by CCHE2D-FLOOD and T_{warn} is the time of public warning. Setting beginning of dam break as time “0”, T_{warn} can be either positive (warning is given after the flood event happens), or negative (warning is given before the flood event happens). Table 2, developed by Graham (1999), is stored in the knowledge base of the decision support system. The fatality rate for each cell is evaluated using this table based on the three parameters: flood severity, escape time, and perception of flood severity. When this number is multiplied by the PAR, an estimation of the potential fatalities in that cell is obtained.

Computation of loss of life is subjected to various uncertainties. DSS-WISE gives the user the possibility of assigning different types of probability distributions (uniform, triangular, Gaussian) to many of the variables used in the estimation of loss of life. Monte-Carlo Simulation is subsequently used to calculate the propagation of uncertainties and compute different statistical moments (expected value, standard deviation, etc).

The urban flood damage tool in DSS-WISE takes into account only direct flood losses in relation to direct physical damage on the residential building stock and industrial buildings. The flowchart of the urban damage tool is provided in Figure 21. CCHE2D-FLOOD computations provide raster files of the map of flood velocities. The information about the residential building stock and industrial buildings may come from urban property surveys, if available, or from existing data sources, such as HAZUS-MH database. If none is available, a classified remote sensing image may also be used along with user assumptions regarding building density and

type. The knowledge base contains both depth and/or velocity versus percent damage relationships and property values, and contents values for different types of buildings. For a given cell, the flood depth and velocity are known. The percent damage for each type of building is determined by combining this information with the corresponding depth and/or velocity versus damage curve.

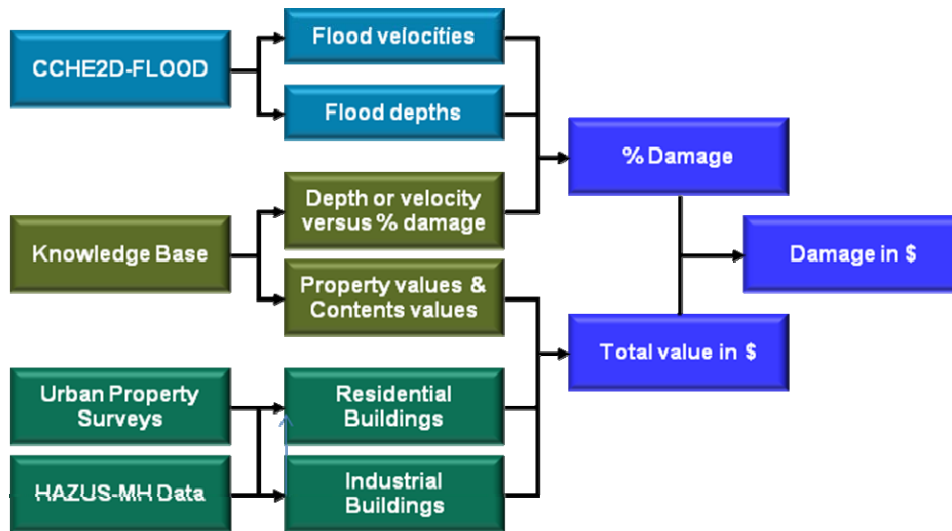


Figure 21. Urban flood damage calculation

The agricultural damage tool in DSS-WISE takes into account only direct flood losses in relation to direct physical damage to crops, farm buildings, and facilities based on procedures used by the U.S. Department of Agriculture, National Resources Conservation Service (NRCS). The flowchart for the computational procedure is shown in Figure 22. The flood damage to farm buildings and farm facilities is a procedure similar to the computation of urban flood damage (right side of the flowchart). In addition, crop damage due to flood must also be calculated. This computation also requires information regarding the time of the event (month of the year) that must be provided by the user.

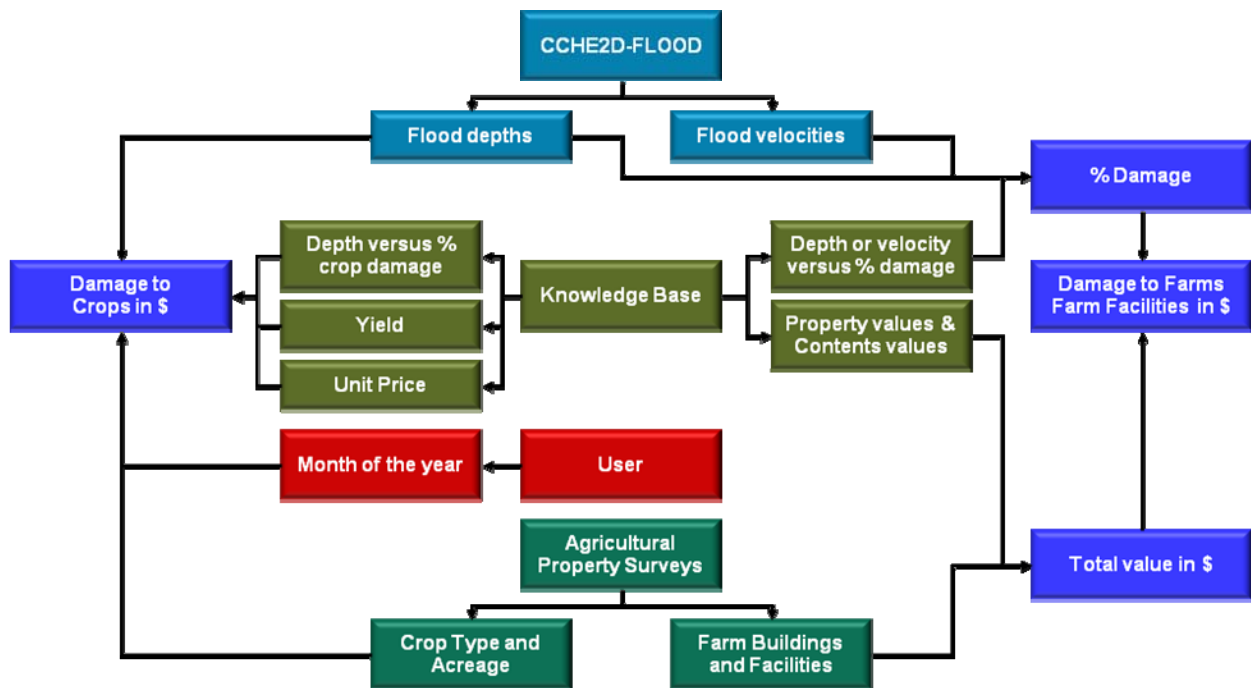


Figure 22. Agricultural damage calculation according to NRCS procedures

The data on crops, farm buildings, and facilities are provided by field surveys or interviews with property owners. It includes the following items: farm/owner name, geographical locations (x/y coordinates), area, crop types, unit crop yield quantities, etc. Crop prices are also obtained for the area of interest. According to the general procedure developed by NRCS, damage calculations are based on stage-yield versus percent damage functions shown in Table 3 for the Northern U.S. The information in Table 3 is derived either from past flood data analysis, or through analytical descriptions of flood damage to various crops considering the possible damage ratio to a given flood depth, crop yield quantity, and the time that a flood occurs. It is interesting to note that negative numbers in the table signify that some flood event could even increase the potential

production return of certain crops. More detailed information on agricultural damage computations in DSS-WISE can be found in Qi et al. (2006) and Altinakar et al. (2008).

Crop and Depth of Flooding (in <i>ft</i>)	Yield	Damage Per Acre as a Percent of Flood-Free Gross Return by Months							
		April	May	June	July	August	September	October	November
<u>Corn</u> <u>Grain</u> 0-2'	75 bu	0	4	30	31	14	9	10	3
	125 bu	0	3	29	32	15	9	10	4
	175 bu	0	3	28	32	15	9	10	4
<u>Corn</u> <u>Grain</u> over 2'	75 bu	0	5	41	60	38	27	23	8
	125 bu	0	4	41	62	39	27	24	8
	175 bu	0	4	39	63	39	28	24	8
<u>Soybeans</u> 0-2'	25 bu	0	3	40	67	64	45	33	10
	40 bu	0	2	40	70	66	46	34	11
	60 bu	0	2	40	71	68	47	35	11
<u>Soybeans</u> over 2'	25 bu	0	4	54	86	86	65	38	11
	40 bu	0	3	53	89	89	67	40	11
	60 bu	0	2	51	91	91	69	40	11
<u>Oats</u> 0-2'	50 bu	15	16	46	54	24	0	0	0
	70 bu	12	0	46	53	21	0	0	0
	90 bu	11	- 9	46	52	20	0	0	0
<u>Oats</u> over 2'	50 bu	23	25	75	81	38	0	0	0
	70 bu	19	0	75	78	33	0	0	0
	90 bu	16	- 14	75	77	31	0	0	0

Table 3. Crop flood damage for the Northern U.S. based on event month, yields, and flood depths

Finally, The Spatial Compromise Tool is a geospatial, multi-criteria decision-making tool that can take into account the spatial distribution of decision criteria. It can be effectively used for comparing flood protection alternatives. A detailed description of this tool as implemented in DSS-WISE can be found in Qi et al. (2005).

CONCLUSIONS

After reviewing the basics of unsteady flow and dam-break hydraulics, some of the scientific and technological gaps in the current practice of dam-break simulation and consequence analysis are identified. In recent years, considerable advances have been made in the development of 1D and 2D shock-capturing upwind finite volume and finite element schemes. This paper has briefly introduced the basic idea behind Godunov type upwind finite-volume methods and provided the names of some popular high resolution TVD schemes. These new numerical techniques, which allow simulation of mixed flow regimes in the same computational domain and handle wetting and drying problems often encountered in dam-break type floods, open up new avenues for better and more realistic dam-break flood simulations. It is also argued that as a result of recent advances in numerical methods, computer hardware and software, and geospatial data technologies, the use of 2D models in engineering practice has now become a cost- and time-effective alternative to classical 1D simulations, which are often pushed beyond their limit of applicability.

As an example, the DSS-WISE Integrated Simulation and Consequence Analysis System for dam-break studies was briefly presented. This integrated system comprises a state-of-the art 2D numerical model and a collection of GIS-based decision support system with pre- and post processing capabilities. The 2D finite-volume numerical model, CCHE2D-FLOOD, uses a shock capturing upwind scheme to simulate the propagation of a flood discharge over complex topography represented by a DEM. Mixed flow regimes are allowed and wetting and drying is handled using a very small water depth everywhere in the domain. CCHE2D-FLOOD is enhanced by implementing a two-sided cut-cell boundary method to represent linear terrain

features that cannot be captured at the resolution level of the DEM. A special version of the cut-cell boundary technique is also used to provide coupled 1D-2D simulations. Some test cases demonstrating these capabilities were presented. The results provided by CCHE2D-FLOOD can be readily imported onto the ArcGIS Platform as raster files. A collection of decision support tools are provided to interface these numerical results with geospatial socio-economic data to evaluate the consequences of the flood event, such as potential loss of life, and urban and agricultural damage. The components of this system were also briefly described.

REFERENCES

- M. S. Altinakar, M. Z. McGrath, Y. Ozeren and H. Omari (2008): “Modeling and Risk Analysis for Floods due to Failure of Water Control Infrastructures”; Proceedings (CD-ROM) of the International Symposium on Uncertainties in Hydrologic and Hydraulic Modeling, Oct 15-20, 2008, Montreal, Canada.
- M. Altinakar, M. McGrath, Y. Ozeren, and E. Miglio (2009a): “Representation of Linear Terrain Features in a 2D Flood Model with Regular Cartesian Mesh”, accepted for oral presentation and publication in the Proceedings of the 2009 World Environmental & Water Resources (EWRI) Congress, ASCE, May 16-23, 2009, Kansas City, Missouri.
- M. Altinakar, M. McGrath, Y. Ozeren, and E. Miglio (2009b): Two-Sided Cut-Cell Boundary Method for Simulating Linear Terrain features and 1D Stream Flows on a 2D Rectangular Mesh”, accepted for oral presentation and publication in the Proceedings of the 33rd International IAHR Biennial Congress, August 9-14, 2009, Vancouver, Canada.

- Bowles, D.S., Anderson, L.R., Glover, T.F. (1998): “The Practice Of Dam Safety Risk Assessment And Management: Its Roots, Its Branches, And Its Fruit”; Proceedings of the 18th USCOLD Annual Meeting and Lecture, Buffalo, New York, August 8-14, 1998.
- Brown, R. J. & Rogers D. C. (1981): “BRDAM Users Manual. Water and Power Resources Services”, US Dept of the Interior, Denver, Colorado, USA
- Chanson, H. (2004): “Hydraulics of Open Channel Flow, An Introduction”, 2nd edition, Elsevier, Butterworth-Heinemann, Amsterdam.
- DHS (2009): “National Infrastructure Protection Plan: Partnering to enhance protection and resiliency”;
- Franz, D.D. and Melching, C.S. (1997): “Full equations (FEQ) model for the solution of the full, dynamic equations of motion for one-dimensional unsteady flow in open channels and through control structures”; U.S. Geological Survey Water-Resources Investigations Report 96-4240, 258 p.
- Froelich, D. C., 1996, “Finite Element Surface-Water Modeling System: Two-Dimensional Flow in a Horizontal Plane”, FESWMS-2DH, Version 2, User’s Manual, Federal Highway Administration, Turner-Fairbank Highway Research Center, McLean, VA
- Froelich, D. (2002): “Users’ Manual for FESWMS Flo2DH: Two-Dimensional Depth-Averaged Flow and Sediment Transport Model”, Release 3
- Frazão, S.S., De Bueger, C., Dourson, V., and Zech, Y. (2002): "Dam-Break Wave Over a Triangular Bottom Sill"; Proceedings River Flow 2002 Conference, Louvain-la-Neuve, Belgium, September 2002, Balkema, Vol. 1, pp. 437-442
- Fread, D.L. (1985): “Channel routing”; in: Anderson, M.G. and Burt, T.P. Editors, 1985. Hydrological Forecasting Wiley, Chichester.

- Fread, D.L. (1993): “NWS FLDWAV Model: The Replacement of DAMBRK for Dam Break Flood Prediction”; Proceedings of 10th Annual Conference of the Association of State Dam Safety Officials, Inc., Kansas City, MO, Sept 26-29, 1993, pp. 177-184.
- Graham, W.J. (1999), “A Procedure for Estimating Loss of Life Caused by Dam Failure”, Report No. DSO-99-06, Dam Safety Office, US Bureau of Reclamation, Denver, CO.
- HEC (2008a): “HEC-RAS (River Analysis System) Hydraulic Reference Manual”, Version 4.0, March 2008, Author: G.B. Brunner, US Army Corps of Engineers, Institute for Water Resources, Hydrologic Engineering Center, Davis, CA.
- HEC (2008b): “HEC-RAS (River Analysis System) User’s Manual”, Version 4.0, March 2008, Author: G.B. Brunner, US Army Corps of Engineers, Institute for Water Resources, Hydrologic Engineering Center, Davis, CA.
- Jorgeson Jeff, Xinya Ying and Woodman Wardlaw (2005): “Two-Dimensional Modeling of Dam Breach Flooding”; Proceedings on CD, US-China Workshop on Advanced Computational Modeling in Hydrosience and Engineering, September 19-21, 2005, Oxford, Mississippi, USA.
- Krishnappan, B.G. and Altinakar, M.S. (2005): “Chapter 139: Numerical modelling of unsteady flows in Rivers”; in Encyclopedia of Hydrological Sciences. p. 2129-2148, Ed. by M.G. Anderson and J.J. McDonnell, John Wiley and Sons, Sussex, England.
- Leal, J.G.A.B.,1 Ferreira, R.M.L, and Cardoso, A.H. (2006): “Dam-Break Wave-Front Celerity”; ASCE, JHE, 132(1), 69-76
- LeVeque, R.J. (1999): “*Numerical Methods for Conservation Laws*”; Birkhäuser Verlag, Basel, Switzerland.
- LeVeque, R.J. (2002): “*Finite Volume Methods for Hyperbolic Problems*”; Cambridge Texts in Applied Mathematics Series, #31, Cambridge University Press.

- Meselhe, E. A. and Holly, F.M. Jr. (1997): “Invalidity of Preissmann Scheme for Transcritical Flow”; ASCE, JHE, 123(7), 652-655.
- E. Miglio, M. S. Altinakar, and Tayfur, G. (2008): “Representation of Linear Terrain Features in 2D Free Surface Models using Cut-Cell Boundary Method”, Proceedings of River Flow 2008, International Conference on Fluvial Hydraulics, Cesme, Izmir, Turkey, September 3-5, 2008.
- Preissmann, A. (1961): “Propagation des Intumescences dans les Canaux et Rivières”; Proceedings of the First Congress of the French Association for Computation, Grenoble, France, 433-442.
- Qi, H., Altinakar, M.S., Ying, X. and Wang, S.S.Y. (2005); “Flood Management Decision Making Using Spatial Compromise Programming with Remote Sensing and Census Block Information”, submitted to XXXI International Association for Hydraulic Research (IAHR) Congress, Seoul, Korea, Sept 2005.
- Qi, H., Altinakar, M.S., and Jeon, Y. (2006): “A Decision Support Tool for Flood Management under Uncertainty Using GIS and Remote Sensing”, Proceedings of 7th International Conference on Hydroscience and Engineering (ICHE 2006), Philadelphia, PA, Sept 2006.
- Ritter, A. (1982): “Die Fortpflanzung de Wasserwellen”; Zeitschrift verein Deutsche Ingenieure, 36(33), 947-954 (in German).
- Toro, E.F. (1999): “*Riemann Solvers and Numerical Methods for Fluid Dynamics*”; 2nd Ed., Springer-Verlag, Berlin, Germany.
- Toro, E.F. (2001): “*Shock-Capturing Methods for Free-Surface Shallow Flows*”; Wiley and Sons Ltd., Chichester, U.K.
- Ying, X. and S.S.Y. Wang (2004): “Two-Dimensional Numerical Simulations of Malpasset Dam-Break Wave Propagation”; Proceedings of 6th International Conference on

Hydroscience and Engineering, Brisbane, Australia, Book of Abstracts Pg. 137-138,

Manuscript on CDROM,, May, 2004.

Ying, X., Sam S.Y. Wang,. and A.A. Khan (2003a): “Numerical Simulation of Flood Inundation

Due to Dam and Levee Breach”; Proceeding of ASCE World Water & Environmental

Resources Congress 2003 (CD-ROM), Philadelphia, USA, June 2003.

Ying, X., A. A. Khan, and S. S. Y. Wang (2004): “An Upwind Conservative Scheme for Saint

Venant Equations”; ASCE-JHE 130(10), pp. 977-987.

Corresponding Author:

Name: Mustafa S. Altinakar
Title: Associate Director and Research Professor
Organization: National Center for Computational Hydrosience and Engineering
The University of Mississippi
Address: NCCHE
Carrier Hall, Room 102
City: University
State: MS
Postal Code: 38677
Country: USA
Phone: 662-915-3783
Fax: 662-915-7796
E-mail: altinakar@ncche.olemiss.edu